Management oriented mathematical modelling of Ria Formosa (South Portugal)

MONOGRAPH

Duarte, P.[1]*, Azevedo, B.[1], Ribeiro, C.[1], Pereira, A.[1], Falcão, M.[2], Serpa, D[2], Bandeira, R.[1] and Reia, J.[3]

[1]Global Change, Energy, Environment and Bioengineering R & D Unit, Faculty of Science and Technology, Fernando Pessoa University, Praça 9 de Abril 349, P-4200 Porto, Portugal. pduarte@ufp.pt

[2]Portuguese Marine Research Institute (IPIMAR), CRIP Sul, Av. 5 de Outubro, 2700 Olhão, Portugal

[3]Parque Natural da Ria Formosa, Centro de Educação Ambiental do Marim, Quelfes, 8700 Olhão, Portugal

Abstract

1 - Ria Formosa is a large (c.a. 100 km^2) mesotidal lagoon system included in a Natural Park, with large intertidal areas and several uses such as fisheries, aquaculture, tourism and nature conservation. Its watersheds cover an area of approximately 864 km^2, with a hydrographic network of small and, mostly, ephemeral rivers.

2 - The Soil and Water Assessment Tool (SWAT model) has been applied to the catchments in order to simulate water discharges to Ria Formosa, providing forcing to a two-dimensional vertically integrated model, implemented with EcoDynamo – an object oriented modelling software – including hydrodynamics, water column and sediment biogeochemistry and growth models for some important benthic species.

3 - The main objectives of this work are to: (i) Analyse model performance in the light of available data; (ii) Evaluate the effects of dredging operations and changes in biomass densities of cultivated clams, on lagoon biogeochemistry and water quality.

4 - This work is part of a larger project where many possible management scenarios are being analysed following concerns expressed by the project end-users – Ria Formosa Natural Park authority.

5 - Results obtained so far suggest that bivalve rearing areas are probably being exploited close to their carrying capacity. Furthermore, it is apparent that some improvement on water quality could be achieved by reducing bivalve densities, without significant losses of harvest yields.

Keywords: Coastal lagoon modelling, Management, Carrying capacity

Introduction

Coastal ecosystems, such as estuaries and coastal lagoons, have been intensively used for many years for fisheries, harbour activities, aquaculture, tourism, nature conservation and as a final destination for wastewater and land drainage, among other things. These coexistent and, in many cases, conflicting uses, turn the management of such ecosystems into a very complex issue, demanding the participation of several different stakeholders and the usage of adequate data management, modelling and decision support tools, covering environmental, economic and social aspects.

The European Water Framework Directive (WFD; EC, 2000/60) introduced important changes on the way water is managed in European Union countries. In the WFD, the close link between watersheds and coastal waters it recognised by defining the "River basin district" – a management unit made up of river networks, groundwaters and associated

coastal waters (EC, 2000/60). This fact is in accordance with an increasing tendency to link watershed, hydrodynamic and water quality models (e.g. Park *et al.*, 2003; Plus *et al.*, 2006). The general approach is to use an watershed model coupled with a lagoon model, with the former producing forcing conditions for the latter in terms of river flows, nutrient and suspended matter loads (Plus *et al.*, 2006).

The involvement of stakeholders has long been recognized as a crucial matter towards sustainable management (e.g. United Nations, 1992; Costanza and Andrade, 1998; Honey, 1999). This work was developed within the European project DITTY (Development of information Technology Tools for the management of Southern European lagoons under the influence of river-basin runoff (EESD Project EVK3-CT-2002-00084). The approach followed within DITTY involves stakeholders and scientists, with the former providing management concerns, constraints, questions and experience-based knowledge to be addressed/developed by the latter, through the usage of information technology tools. The mentioned tools consist of (i) databases (DB) and geographical information systems (GIS) for data storage, management and visualisation; (ii) mathematical models, for the watersheds draining to the coastal ecosystems and for the lagoons themselves; (iii) decision support systems (DSS), to integrate model results, environmental and socio-economic data into the process of decision making. Models are mostly used to analyse several possible management scenarios to provide some sound bases for management decisions.

This paper concerns an important part of the development of the DITTY project at one of its study sites – Ria Formosa (South Portugal) – namely, testing of a mathematical model and presentation and discussion of results concerning part of a scenario analysis previously defined with end-users involved in Ria Formosa Natural Park management. Therefore, the objectives of this work are to:

(i)   Analyse model performance in the light of available data;

(ii)   Evaluate the effects of dredging operations and changes in biomass densities of cultivated clams, on lagoon biogeochemistry and water quality.

Methodology

Site description

Ria Formosa is a shallow mesotidal, eurihaline lagoon located at the south of Portugal (Algarve coast) with a wet area of 105 km^2 (Fig. 1), classified as "Coastal waters" (INAG, 2005) within the scope of the Water Framework Directive (EC, 2000/60). The lagoon has several channels and a large intertidal area which corresponds roughly to 50% of the total area, mostly covered by sand, muddy sand-flats and salt marshes. The intertidal area is exposed to the atmosphere for several hours, over each semi-diurnal tidal period, due to its gentle slopes. Tidal amplitude varies from 1 to 3.5 meters and the mean water depth is 3.5 m (Falcão *et al.*, 2003). This coastal lagoon is a Natural Park, where several institutions have management responsibilities such as the Portuguese Nature Conservation Institute, some municipalities and the Navy.

Ria Formosa watershed has a northern boundary defined by the Caldeirão mountain range, with a maximum and an average altitude of 522 and 112 m, respectively, an area of 864.26 km^2 and a perimeter of 165.99 km (Fig. 1) (MAOT, 2000). Its rivers, mostly ephemeral, drain perpendicular to the South towards the Atlantic Ocean. Average annual precipitation values are between 600 and 800 mm, the wettest month is December with about 17% of total annual precipitation, followed by November and January (about 15%). The driest months are July and August with less than 1% of annual precipitation.

Lagoon modelling

The model was implemented using EcoDynamo (Pereira and Duarte, 2005). EcoDynamo uses Object Oriented Programming (OOP) (Borland, 1988) to relate a set of "ecological" objects by means of a server or shell, which allows these to interact with each other, and displays the results of their interaction. Both the EcoDynamo shell

and the objects have been programmed in C^{++} for WindowsTM. There are different objects to simulate hydrodynamic, thermodynamic and biogeochemical processes and variables. The shell interface allows the user to choose among different models and to define the respective setups – time steps, output formats (file, graphic and tables), objects to be used and variables to be visualised.

The model implemented in this work is a two-dimensional vertically integrated model based on a finite difference staggered grid (100 m resolution). The hydrodynamic object and respective validation were described previously (cf. – Duarte *et al.*, 2005; Duarte *et al.*, in press). It calculates the velocity field with the equations of motion and the equation of continuity (Knauss, 1997), solving the transport equation for all pelagic variables:

$$\frac{dS}{dt} + \frac{\partial(uS)}{\partial x} + \frac{\partial(vS)}{\partial y} = A_x\frac{\partial^2 S}{\partial x^2} + A_y\frac{\partial^2 S}{\partial y^2} + Sources - Sinks \quad (1)$$

where,

u and v - current speeds in x (West-East) and y (South-North) directions (ms^{-1}); A – Coefficient of eddy diffusivity (m^{2}s^{-1}); S – conservative (Sources and Sinks are null) or a non conservative variable in the respective concentration units.

The biogeochemical model provides the values for the Sources and Sinks terms of equation 1 at each grid cell.

Given the large intertidal areas of Ria Formosa, the model includes a wet-drying scheme that prevents any grid cell from running completely dry, avoiding numerical errors (Duarte *et al.*, 2005; Duarte *et al.*, in press). In order to increase model speed, the following steps were taken: (i) To subdivide Ria Formosa in two subsystems – the western and the eastern Ria - as described in a previous report (Duarte *et al.*, 2005) (cf. Fig. 1); (ii) To run only the hydrodynamic part of the model, save the results and "rewind" them later to provide the hydrodynamic forcing for the biogeochemical simulations and (iii) To use a multi- processing version of EcoDynamo (Pereira *et al.*, 2006).

Biogeochemical model description and implementation

The objects used in the present model are listed in Table 1 and described below. Differential equations used for dissolved substances, pore water and sediment variables, suspended matter and macroalgae, seagrasses and bivalves are shown in Tables 2 to 5. Part of these equations (those concerning pelagic state variables), represent the sources-sinks terms of Equation 1. The corresponding rate equations are presented in Tables 6 to 9. Model parameters are listed in Table 10.

The model includes the pelagic and the benthic compartment as well as their interactions. Salt marsh object acts merely as a nitrate sink and an ammonium and particulate organic matter source, according to experimental data obtained by Falcão (unpublished). It is assumed that nitrate-nitrogen input equals ammonium-nitrogen output, minus the fraction converted to particulate organics and used as one of the calibration parameters. This influx/outflux occurs along the salt marsh boundaries (Fig. 2). The model is also forced by WTP discharges (WTP location shown in Fig. 1) regarding suspended matter and nutrient loads.

Hydrodynamic object

The hydrodynamic object was described in previous works (Duarte *et al.*, 2005; Duarte *et al.*, in press). It is forced by tidal height variability at the sea boundaries. It may also be wind forced, although this effect is negligible in Ri Formosa by comparison with tidal forcing and was not included in current simulations. This object allows the output of time integrated current velocities and flow values for each grid cell. These outputs may later be used to run the remaining biogeochemical objects without the necessary calculation overhead of the hydrodynamic processes. Therefore, a specific transport object was implemented in EcoDynamo just to handle the time series calculated by the hydrodynamic object. This transport object computes the equation of continuity, as described in Duarte *et al.* (2005) and Duarte *et al* (in press) and the transport equation (1) for all pelagic variables of the other objects.

Wind object

This object returns wind speed forcing average values to the water temperature object. These values are then used to calculate water heat losses through evaporation.

Air temperature object

This object reads air temperature values and returns them to the water temperature object, to be used to calculate sensible heat exchanges between the water and the atmosphere.

Light intensity and water temperature objects

Light intensity and water temperature are calculated by a light and a water temperature object using standard formulations described in Brock (1981) and Portela and Neves (1994). Submarine light intensity is computed from the Lambert-Beer law. The water light extinction coefficient is computed by the suspended matter object (see below and equation 30).

Sediment biogeochemistry object

The benthic compartment is divided in two vertical layers - the upper layer with an initial height of 0.3 cm and a lower layer with an initial height of 10 cm. Sediment biogeochemistry, water-sediment and sediment-sediment exchanges (across the two layers) by diffusion are calculated with equations and parameters described in Chapelle (1995). The height of the top layer may increase or decrease according to the net result of deposition and resuspension (see below Suspended matter object). The initial sediment distribution is depicted in Fig. 3, with sediments classified as mud, muddy sand, sandy mud and sand.

Dissolved substances object

The concentrations of dissolved inorganic nitrogen (DIN) - ammonium, nitrite and nitrate, inorganic phosphorus and oxygen in each of the model grid cells are calculated as a function of biogeochemical and transport processes, including exchanges with the sea, loads from rivers and waste water treatment plants (WTPs), and exchanges across the sediment water interface (Table 2). These variables are also calculated in pore water (Table 3 and above). Both the nitrogen and phosphorus cycles are simulated using equations and parameters described in Chapelle (1995). The only

exception is the raeration coefficient, calculated as a function of wind speed, following Burns (2000). Phytoplankton and macroalgae remove nutrients from flowing water. *Zostera noltti* also removes nutrients from pore water through the roots (Plus *et al.*, 2003).

Suspended matter object

This object computes total particulate matter (TPM in mg L^{-1}) and particulate organic matter (POM in mg L^{-1}) from deposition and resuspension rates, the exchanges with the sea and with other boxes (transport by the hydrodynamic object), and the net contribution of phytoplankton biomass (Table 4). POM mineralization is calculated as in Chapelle (1995), returning the resulting inorganic nitrogen and phosphorus to the dissolved substances object.

Deposition of TPM in each grid cell is based on sinking velocity and cell depth (returned by the hydrodynamic object). Sinking velocity is considered constant but with different values for inorganic and organic matter (calibrated) (Tables 4, 6 and 10).

Resuspension of TPM in each grid cell is calculated as a function of current velocity and bottom drag, returned by the hydrodynamic object (Table 6). Below a critical velocity value, resuspension does not occur. Above a certain threshold for the product of bottom drag times current velocity (velocity shear), resuspension is assumed constant. This is to avoid unrealistically high resuspension rates. This object is partly based on a Stella (HPS, 1997) model developed by Grant and Bacher (unpublished).

The light extinction coefficient (m^{-1}) is calculated from an empirical relationship with TPM (Equation 30 in Table 7), obtained from historical data for Sungo Bay (Bacher, pers com).

Phytoplankton object

Phytoplankton productivity is described as a function of light intensity (depth integrated Steele's equation) (Steele, 1962), temperature and a limiting nutrient – nitrogen or phosphorus (Table 7). In this model, phytoplankton is represented through chlorophyll, carbon, and nitrogen pools. This allows the necessary

bookkeeping calculations on cell quotas. Traditional approaches with models based solely on nitrogen or phosphorus do not allow these computations. Internal cell quotas are then used to limit carbon fixation through photosynthesis. A nutrient limiting factor in the range 0 – 1 is calculated both for internal nitrogen and phosphorus. The lowest obtained value is then multiplied by light and temperature limited photosynthesis following Liebig's law of minimum.

Nutrient uptake and limitation is described as a three-stage process (Table 7, equations 33-38), following Jørgensen and Bendoricchio (2001) :

(i)   The uptake of nitrogen and phosphorus is dependent on their concentration in the water, on their cell quotas and on the ranges of their cellular ratios;

(ii)   After uptake, nutrients accumulate in the cells;

(iii)   Internal nutrient concentration is used to limit phytoplankton productivity.

A Michaelis-Menten equation is used to relate nutrient uptake with their concentration in the water, following several authors (e.g. Parsons *et al.*, 1984; Ducobu *et al.*, 1998; Jørgensen and Bendoriccchio, 2001). The parameters of this equation are the half-saturation constant and the maximum uptake rate. These were taken from the literature, within the range of measured values (Cochlan and Harrison, 1991; Jørgensen et al., 1991). The Michaelis-Menten equation is not the only regulating mechanism of nutrient uptake, which is also constrained by current cell quotas to avoid values outside ranges reported in the literature, to guarantee homeostasis. When N:P ratios are outside limits currently measured, N or P uptake is constrained. Nitrogen uptake rate is calculated first for ammonium nitrogen and then for nitrite + nitrate, reducing their uptake proportionally to ammonium uptake. This is based on the usual assumption that ammonium is the preferred nitrogen source for phytoplankton (Parsons et al., 1984). Phytoplankton respiration is based on the model of Langdon (1993) (Table 7, equations 40 and 41).

Enteromorpha spp. and Ulva spp. Objects
These objects were computed as described in

Solidoro *et al.* (1997) and Serpa (2004) (Tables 5 and 8).

Zostera noltti object
This object computes *Z. noltii* photosynthesis, respiration, nutrient uptake, translocation and reclamation, growth, mortality and recruitment as described in Plus et al. (2003), except for some modifications described below. In Plus et al. (2003), growth is calculated without considering any limit to plant individual weight or size. Therefore, the model may produce biomass standing stocks and plant densities that imply unrealistically large individual sizes. This can be avoided by careful calibration. However, in the present model it was decided to create some mechanisms to avoid this potential problem. This was done by defining an asymptotic individual weight for Zostera leaves. Any biomass production leading to growth above that asymptotic value is released as detritus to the suspended matter object. *Z. noltii* parameters differing from those reported in Plus et al. (2003) are listed in Table 10, using the same symbols of those authors.

Ruditapes decussatus object
Differential and rate equations for the clam object are depicted in Tables 5 and 9, respectively. Parameters are listed in Table 10. Rate equations were obtained from ecophysiology data reported in Sobral (1995). The general approach to simulate bivalve feeding and growth is similar to other works (e.g. Raillard *et al.*, 1993; Raillard and Ménesguen, 1994; Ferreira *et al.*, 1998; Duarte *et al.*, 2003). Clearance rate is computed from an empirical relationship with TPM, water temperature and oxygen concentration. Temperature limitation is calculated from a direct linear relationship with water temperature, until 20ºC, and an inverse linear relationship, above that value. Oxygen limitation is calculated as a linear function of oxygen saturation, when this is below 28% saturation (hypoxia conditions). Ingestion is calculated from clearance and pseudofaeces production rate. Absorption is calculated from ingestion and faeces production and the usual asymptotic relationship with ingested organics (e.g. Hawkins *et al.*, 1998). Scope for growth is

calculated from absorption and metabolism. Respiration is calculated as a function of oxygen saturation.

When saturation is below 33 %, respiration rate decreases (Sobral, 1995). Allometric relationships are used to correct for bivalve weight, since all physiologic rates are calculated for a standard animal with 1 g dry meat weight.

Model setup

In what concerns pelagic variables, the model was initialized with the same concentrations over all model domain, under the assumption that local and exchange processes would produce a rapid change (within a few hours) of initial conditions, which was the case. Regarding pore water and sediment variables, uniform values were used to initialize conditions in similar sediment types. These were defined as sand, sand-muddy, muddy-sand and muddy. Water, pore water and sediment variable values were obtained from a database available at the DITTY project web site (www.dittyproject.org), as well as forcing conditions in terms of water quality variables in river water flowing into the Ria and at sea boundaries. River flows were simulated with the SWAT model (Guerreiro and Martins, 2005; Duarte et al, in press). Sediment types and distribution of benthic variables were obtained from a GIS developed partly during the same project (Rodrigues *et al.*, 2005). Figs 2 – 4 summarize distribution of sediment types and benthic variables.

Model testing

Validation of the hydrodynamic sub-model was carried out before (Duarte et al., 2005; Duarte al, submitted) and will not be discussed in this work. The same applies to the SWAT model application used to force the lagoon model at river boundaries (Guerreiro and Martins, 2005). Regarding the biogeochemical sub-model, a significant part of model parameters was taken from the literature: e.g. water column and sediment biogeochemistry, seagrass, macroalgal and some phytoplankton parameters from Chapelle (1995), Solidoro *et al.* (1997), Plus et al. (2003), Serpa (2004) and Falcão (1997), respectively. Some parameters were calibrated with a zero dimensional (0D) version of the

model. Several simulations were carried out with full model complexity to check model consistency (sensu Kooijman, 2003) and if predictions remained within reasonable limits.

For the purposes of model calibration and validation it is important to have data on boundary and forcing conditions collected simultaneously with data inside the lagoon. Most of the data available for Ria Formosa does not fulfil these requirements – for some years there is data collected inside the lagoon but not at the sea and river boundaries and vice-versa. Fortunately, there is a relatively old data set for 1992 (Falcão, 1996) that includes nutrient data inside and outside (at the sea boundary) the lagoon sampled at a number of stations depicted in Fig 1. This data set was used to test the model. This test simulation will be hereafter referred as the "standard simulation". However, given the fact that lagoon bathymetry changes very rapidly and that the bathymetry used in the model was obtained in a relatively recent survey (conducted by the Portuguese Hydrographic Institute in 2000), the comparison between observed and predicted data should be carried out with caution.

Scenario analysis

Within the DITTY project, scenarios were defined between end-users and scientists. In the case of Ria Formosa, end-users involved were technicians working at the Natural Park Authority. Scenarios concern mostly bathymetry modifications, related to dredging operations, changes in bivalve rearing areas and densities, changes in salt marsh areas and in number and performance of WTPs. The former were partly discussed previously (Duarte *et al.*, 2006; Duarte *et al.*, submitted).

This work focus on the effect of dredging operations and changes in the density of cultivated clams on lagoon biogeochemistry, according to the objectives stated before (cf. – Introduction). To fulfil the mentioned objectives, simulations were carried out in order to simulate a particular dredging operation, hereafter referred as the Ramalhete (average depth increased by 0.5 m) and Olhão (doubling average depth) scenarios (Fig. 5), and compared with the standard one. Comparisons were made

on the basis of average values for several variables, integrated over a period of one year. Similarly, simulations were run with various bivalve densities – ½, 2 and 3 times normal density, to simulate different seeding densities of 0.5, 1, 2 and 3 kg (Fresh Weight (FW)) m^{-2}, respectively. Comparisons were made on the basis of average values for several variables, integrated over a period of half a year. This period corresponds to the time necessary for bivalves to reach the commercial size, when

seeded in January with an individual weight of 0.12 g meat dry weight. These simulations correspond to part of the scenario analysis mentioned in the previous paragraph.

The comparison between the results obtained under different scenarios (potential management options) was made using the IFREMER water and sediment quality classification scheme (e.g. Austoni *et al.*, 2004). This allows a simple assessment of the impact of each scenario on water and sediment quality.
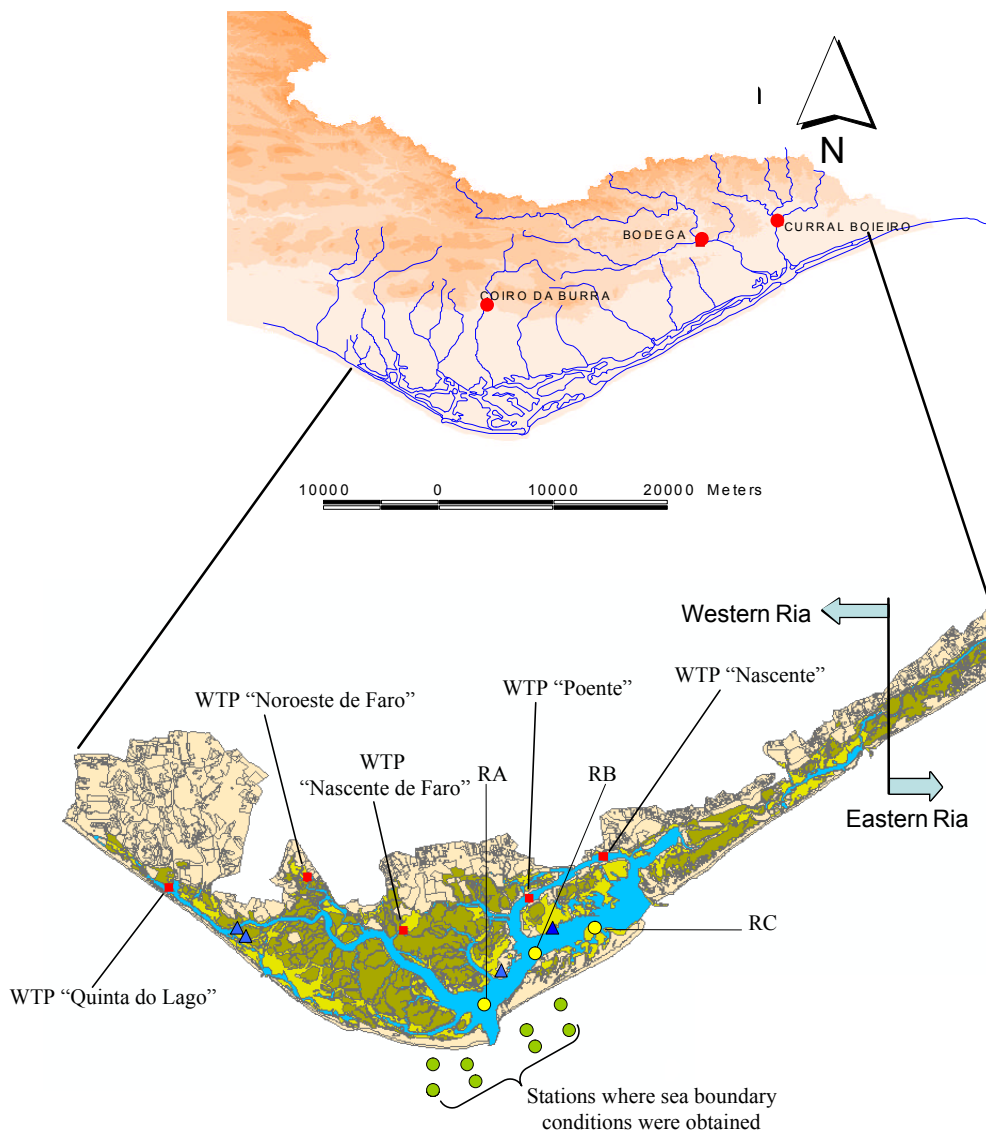
Figure 1 –Ria Formosa coastal lagoon and its watersheds with stream gauge stations shown as red dots (upper map) – used to calibrate/validate the SWAT model application (Guerreiro and Martins, 2005), water quality stations inside - RA, RB and RC (yellow dots), used to calibrate/validate the biogeochemical model (this work) - and, outside - (green dots), used to derive boundary conditions for the model - the lagoon and sediment and pore water quality stations (triangles).The vertical line in the lower image separates the "Western" from the "Eastern" Ria, the former corresponding to the model domain (see text). Also shown the location of the WTP plants (red squares).

Table 1 – EcoDynamo objects implemented for Ria Formosa and respective variable outputs (see text).

Object type	Object name	Object outputs
Objects providing forcing functions	Wind object	Wind speed
	Air temperature object	Air temperature
	Water temperature object	Radiative fluxes and balance between water and atmosphere and water temperature
	Light intensity object	Total and photosynthetically active radiation (PAR) at the surface and at any depth
	Tide object	Tidal height
	Salt marsh object	Nitrate and ammonium fluxes
Objects providing state variables	Hydrodynamic 2D object	Sea level, current speed and direction
	Sediment biogeochemistry object	Pore water dissolved inorganic nitrogen (ammonia, nitrate and nitrite), inorganic phosphorus and oxygen, sediment adsorbed inorganic phophorus, organic phosphorus, nitrogen and carbon
	Dissolved substances object	Dissolved inorganic nitrogen (ammonia, nitrate and nitrite), inorganic phosphorus and oxygen
	Suspended matter object	Total particulate matter (TPM), particulate organic matter (POM), carbon (POC), nitrogen (PON),phosphorus (POP) and the water light extinction coefficient
	Phytoplankton object	Phytoplankton biomass, productivity and cell nutrient quotas
	Enteromorpha sp. object	Macroalgal biomass, productivity and cell nutrient quotas
	Ulva sp. object	Macroalgal biomass, productivity and cell nutrient quotas
	Zostera noltti object	Macrophyte biomass and numbers, cell nutrient quotas and demographic fluxes
	Clams *(Ruditapes decussatus)* object	Clam size, biomass, density, filtration, feeding, assimilation and scope for growth

Table 2 – General differential equations for water column dissolved inorganic nitrogen, phosphorus and oxygen. The subscripts i and j refer to the line and columns of the model grid. These differential equations only describe changes due to non-conservative processes and provide the sources-sinks terms of Equation 1. The load terms refer to loads along the sea, river and land boundaries.

Water column ammonium (NH$_4$) (μmol N l^{-1})		
$\dfrac{d\,NH_{4ij}}{dt} = PONMinerW_{ij} - NitrificationW_{ij} + DeNitrificationW_{ij}$		
$\pm SedWaterDiffusionNH4_{ij}$		(2)
$+ BIVExcrNH4_{ij} - PhyUpNH4_{ij} - EntUpNH4_{ij} - UlvUpNH4_{ij} - ZosUpNH4_{ij}$		
$+ loadsNH4_{ij}$		
Mineralization, nitrification and denitrification as in Chapelle (1995).		
$PONMinerW_{ij}$	Water column particulate organic nitrogen mineralization	
$NitrificationW_{ij}$	Water column nitrification	
$DeNitrificationW_{ij}$	Water column denitrification	
$SedWaterDiffusionNH4_{ij}$	Sediment-water diffusion	μmol N l^{-1} time^{-1}
$BIVExcrNH4_{ij}$	Clams excretion	
$PhyUpNH4_{ij}$	Uptake by phytoplankton	
$EntUpNH4_{ij}$	Uptake by *Enteromorpha sp.*	
$UlvUpNH4_{ij}$	Uptake by *Ulva sp.*	
$ZosUpNH4_{ij}$	Uptake by *Zostera noltii* leaves	
$loadsNH4_{ij}$	Nitrogen loads	
Water column nitrate+nitrite (NO) (μmol N l^{-1})		
$\dfrac{d\,NO_{ij}}{dt} = NitrificationW_{ij} - DenitrificationW_{ij} \pm SedWaterDiffusionNO_{ij}$		
$- PhyUpNO_{ij} - EntUpNO_{ij} - UlvUpNO_{ij} - ZosUpNO_{ij}$		(3)
$+ loadsNO_{ij}$		
The fluxes for the uptakes have the same prefix as for ammonia to indicate the species or species group responsible for each uptake. Their units are μmol N l^{-1} time^{-1}.		
Water column phosphate (PO4) (μmol P l^{-1})		
$\dfrac{d\,PO_{4ij}}{dt} = POPMinerW_{ij} \pm SedWaterDiffusionPO4_{ij}$		
$- PhyUpPO4_{ij} - EntUpPO4_{ij} - UlvUpPO4_{ij} - ZosUpPO4_{ij}$		(4)
$+ loadsPO4_{ij}$		
The fluxes for the uptakes have the same prefix as for ammonia and nitrate to indicate the species or species group responsible for each uptake. Their units are μmol P l^{-1} time^{-1}.		
$POPMinerW_{ij}$	Water column particulate organic phosphorus mineralization	

Table 2 – Continued- General differential equations for water column dissolved inorganic nitrogen, phosphorus and oxygen. The subscripts i and j refer to the line and columns of the model grid. These differential equations only describe changes due to non-conservative processes and provide the sources-sinks terms of Equation 1. The load terms refer to loads along the sea, river and land boundaries.

Water column dissolved oxygen (DO) (mg O_2 l^{-1})

$$\frac{dDO_{ij}}{dt} = \pm SedWaterDiffusion_{ij} + Kar\left(DOsat_{ij} - DO_{ij}\right)$$
$$-BIVResp_{ij} + PhyPHOT_{ij} - PhyResp_{ij}$$
$$+EntPHOT_{ij} - EntResp_{ij}$$
$$+UlvPHOT_{ij} - UlvResp_{ij} \qquad\qquad (5)$$
$$+ZosPHOT_{ij} - ZosResp_{ij}$$
$$-NitrificationConsW_{ij} - MineralizationConsW_{ij}$$

Raeration coefficient calculated as a function of wind speed as in Burns (2000). Oxygen consumption by nitrification and mineralization as in Chapelle (1995) and Chapelle et al. (2000).

Kar	Gas transfer/raeration coefficient	time^{-1}
$DOsat_{ij}$	Dissolved oxygen saturation concentration	mg O_2 l^{-1}
$BIVResp_{ij}$	Bivalve respiration	
$PhyPHOT_{ij}$	Phytoplankton photosynthesis	
$PhyResp_{ij}$	Phytoplankton respiration	
$EntPHOT_{ij}$	*Enteromorpha sp.* photosynthesis	
$EntResp_{ij}$	*Enteromorpha sp.* respiration	
$UlvPHOT_{ij}$	*Ulva sp.* photosynthesis	mg O_2 l^{-1}time^{-1}
$UlvResp_{ij}$	*Ulva sp.* respiration	
$ZosPHOT_{ij}$	*Zostera noltii* photosynthesis	
$ZosResp_{ij}$	*Z. noltii* above ground respiration	
$NitrificationConsW_{ij}$	Consumption by water column nitrification	
$MineralizationConsW_{ij}$	Consumption by water column mineralization	

Table 3 - General differential equations for pore water variables – pore water ammonium, nitrate+nitrite, phosphate and oxygen – and sediment variables – organic carbon, nitrogen and phosphorus. The subscripts i and j refer to the line and columns of the model grid.

Pore water ammonium (NH$_4$s) (mmol N l^{-1})

$$\frac{dNH_{4s}ij}{dt} = \frac{OrgNMinerS_{ij}SedWaterRatio_{ij}}{NAtomicMass} - NitrificationS_{ij} + DeNitrificationS_{ij}$$
$$\pm SedWaterDiffusionNH4_{ij} - ZosRootNH4S_{ij} \qquad\qquad (6)$$

$OrgNMinerS_{ij}$	Mineralization of sediment organic nitrogen	µg g^{-1} N time^{-1}
$SedWaterRatio_{ij}$		g l^{-1}
$NitrificationS_{ij}$	Pore water nitrification	
$DeNitrificationS_{ij}$	Pore water denitrification	
$SedWaterDiffusionNH4_{ij}$	Sediment-water diffusion	µmol N l^{-1} time^{-1}
$ZosRootUpNH4Ss_{ij}$	Uptake by *Zostera noltii* roots	

Table 3 – Continued - General differential equations for pore water variables – pore water ammonium, nitrate+nitrite, phosphate and oxygen – and sediment variables – organic carbon, nitrogen and phosphorus. The subscripts i and j refer to the line and columns of the model grid.

Pore water nitrate+nitrite (NOs) (mmol N l⁻¹)

$$\frac{d\,NOs_{ij}}{dt} = NitrificationS_{ij} \pm SedWaterDiffusionNOs_{ij} - DenitrificationS_{ij} \qquad (7)$$

Nitrification and denitrification as in Chapelle (1995).

Pore water phosphate (PO₄s) (mmol N l⁻¹)

$$\frac{d\,PO_{4s}ij}{dt} = \frac{OrgPMinerS_{ij}SedWaterRatio_{ij}}{PAtomicMass} \pm SedWaterDiffusion_{ij} \qquad (8)$$
$$- SedimentAdsorption_{ij} + SedimentDesorption_{ij} - ZosRootUpPO4S_{ij}$$

Adorption and desorption as in Chapelle (1995).

$OrgPMinerS_{ij}$	Mineralization of sediment organic phosphorus	µg g⁻¹ N time⁻¹
$ZosRootUpNH4Ss_{ij}$	Uptake by *Z. noltii* roots	µmol P l⁻¹ time⁻¹

Pore water oxygen (DO) (mg l⁻¹)

$$\frac{d\,DO_{ij}}{dt} = \pm SedWaterDiffusion_{ij} - ZosRootResp_{ij} \qquad (9)$$
$$- NitrificationConsS_{ij} - MineralizationConsS_{ij}$$

$ZosRootResp_{ij}$	*Z. noltii* below ground respiration	
$NitrificationConsS_{ij}$	Consumption by pore water nitrification	mg O₂ l⁻¹time⁻¹
$MineralizationConsS_{ij}$	Consumption by pore water mineralization	

OrgN (mg N g⁻¹)

$$\frac{dOrgN_{ij}}{dt} = DetrDepN_{ij} + PhySetN_{ij} - OrgNMinerS_{ij} \qquad (10)$$

$DetrDepN_{ij}$	Deposition of particulate nitrogen	
$PhySetN_{ij}$	Settling of phytoplankton cells	µg N g⁻¹ time⁻¹

OrgP(mg P g⁻¹)

$$\frac{dOrgP_{ij}}{dt} = DetrDepP_{ij} + PhySetP_{ij} - OrgPMinerS_{ij} \qquad (11)$$

$DetrDepP_{ij}$	Deposition of particulate nitrogen	
$PhySetP_{ij}$	Settling of phytoplankton cells	µg P g⁻¹ time⁻¹

Adsorbed PO₄ (mg P g⁻¹)

$$\frac{d\,PO_{4Ads}ij}{dt} = \left(SedimentAdsorption_{ij} - SedimentDesorption_{ij} \right)\frac{PAtomicMass}{SedWaterRatio_{ij}} \qquad (12)$$

(µg P g⁻¹ time⁻¹)

Table 4 – General differential equations for suspended matter. The subscripts i and j refer to the line and columns of the model grid. These differential equations only describe changes due to non-conservative processes and provide the sources-sinks terms of Equation 1. The load terms refer to loads along the sea and river boundaries.

Total (TPM) and organic (POM) particulate matter (mg l^{-1})

$$\frac{dTPM_{ij}}{dt} = TPMDep_{ij} - TPMResus_{ij} + PHYTONPP_{ij} - POMMiner_{ij} + TPMLoads_{ij} \quad (13)$$

$$\frac{dPOM_{ij}}{dt} = POMDep_{ij} - POMResus_{ij} + PHYTONPP_{ij} - POMMiner_{ij} + POMLoads_{ij} \quad (14)$$

(following Duarte et al. (2003))

$TPMDep_{ij}$	TPM Deposition rate	
$TPMResus_{ij}$	TPM Resuspension rate	
$PHYTONPP_{ij}$	Net Phytoplankton Production (in dry weight)	
$TPMLoads_{ij}$	TPM loads	mg l^{-1} time^{-1}
$POMDep_{ij}$	POM Deposition rate	
$POMResus_{ij}$	POM Resuspension rate	
$POMMiner_{ij}$	POM mineralization	
$POMLoads_{ij}$	POM loads	

* - POM and POM fluxes are expressed in POM mass, Carbon, Nitrogen and Phosphorus units

Phytoplankton (mg C l^{-1})*

$$\frac{dPHY_{ij}}{dt} = PHY_{ij}(PHYGPP_{ij} - PHYExud_{ij} - PHYResp_{ij} - PHYMort_{ij}) -$$

$$Gb_{ij}BIV_{ij}conv + PHYLoads_{ij} \quad (15)$$

*For output, phytoplankton biomass is converted to Chlorophyll, assuming a Chlrophyll / Carbon ratio of 0.02 (Jørgensen et al., 1991)

$PHYGPP_{ij}$	Gross primary productivity	
$PHYExud_{ij}$	Exudation rate	
$PHYResp_{ij}$	Respiration rate	time^{-1}
$PHYMort_{ij}$	Mortality rate	
Gb_{ij}	Bivalve grazing rate	
$BIV_{ij}conv$	Bivalve biomass converted to carbon	
$PHYLoads_{ij}$	Phytoplankton loads	µg C l^{-1}time^{-1}

Table 5 - General differential equations for benthic variables. The subscripts *i* and *j* refer to the line and columns of the model grid.

Enteromorpha sp (g DW m^{-2})

$$\frac{dENT_{ij}}{dt} = ENT_{ij}(ENTGPP_{ij} - ENTResp_{ij} - ENTMort_{ij}) \quad (18)$$

$ENTGPP_{ij}$	Gross primary productivity	g DW m-2 time-1
$ENTResp_{ij}$	Respiration rate	time-1
$ENTMort_{ij}$	Mortality rate	time-1

Ulva sp. (g DW m^{-2})

$$\frac{dULV_{ij}}{dt} = ULV_{ij}(ULVGPP_{ij} - ULVResp_{ij} - ULVMort_{ij}) \quad (19)$$

$ULVGPP_{ij}$	Gross primary productivity	g DW m-2 time-1
$ULVResp_{ij}$	Respiration rate	time-1
$ULVMort_{ij}$	Mortality rate	time-1

Zostera noltii (g DW m^{-2})

Variables and equations as described in Plus et al. (2003)

Ruditapes decussatus (g DW m^{-2})

$$\frac{dBIVB_{ij}}{dt} = BIVDens_{ij}(BIVAbsor_{ij} - BIVResp_{ij} - BIVExcr_{ij} - BIVMort_{ij}) \quad (20)$$

$$\frac{dBIVDens_{ij}}{dt} = -\mu BIVDens_{ij} + BIVSeed_{ij} - BIVHarv_{ij} \quad (21)$$

$BIVDens_{ij}$	Density	ind. m-2
$BIVAbsor_{ij}$	Absorption rate	
$BIVResp_{ij}$	Respiration rate	g DW ind-1 time-1
$BIVExcr_{ij}$	Excretion rate	
$BIVMort_{ij}$	Mortality rate	
$BIVSeed_{ij}$	Seeding rate	g DW m-2 time-1
$BIVHarv_{ij}$	Harvest rate	
m	Mortality rate	time-1

<div align="center">

Table 6 – Equations for suspended matter rate processes (see text).

</div>

TPM and POM

$$TPMDep_{ij} = SinkingVelocity_{ij} \frac{TPM_{ij}}{Depth_{ij}} \tag{22}$$

$$TPMResus_{ij} = Erate.VelocityShear_{ij} \tag{23}$$

$$if \sqrt{Drag}\left|CurrentVelocity\right| < CritSpeed \quad then$$
$$VelocityShear_{ij} = 0 \quad else$$

$$VelocityShear_{ij} = \min \begin{pmatrix} \dfrac{0.02^2}{(CritSpeed)^2} - 1.0, \\[2ex] \dfrac{\left(\sqrt{Drag}\left|CurrentVelocity\right|\right)^2}{(CritSpeed)^2} - 1.0 \end{pmatrix} \tag{24}$$

0.02 – Threshold value to avoid very high resuspension rates (calibrated)

$$POMDep_{ij} = TPMDep_{ij} \frac{POM_{ij}}{TPM_{ij}} \tag{25}$$

$$POMResus_{ij} = TPMResus_{ij} \frac{POM_{ij}}{TPM_{ij}} \tag{26}$$

$$Drag = \frac{gn^2}{Depth^{1/3}} \text{ (calculated by the hydrodynamic object)} \tag{27}$$

n	Manning coefficient	
g	Gravity	m s^{-2}
$CritSpeed$	Velocity threshold for resuspension	m s^{-1}

Table 7 – Equations for phytoplankton rate processes. Each rate is multiplied by corresponding carbon, nitrogen or phosphorus stocks to obtain fluxes (see text).

Processes	Equations	Units
Vertically integrated (light limited productivity, from Steele's equation (Steele, 1962))	$$P_{g(I)} = P_{max} \frac{\exp}{kz}\left(exp\left(-\frac{I_z}{I_{opt}}\right) - exp\left(-\frac{I0}{I_{opt}}\right)\right) \quad (28)$$ where, P_{max} – Maximum rate of photosynthesis; I_{opt} – Optimal light intensity for photosynthesis; I_z – Light intensity at depth z;	time^{-1}
Light intensity at box depth	$$I_z = I_0 \exp(-kz) \quad (29)$$	μ E m^{-2} time^{-1}
Light extinction coefficient	$$k = 0.0243 + 0.0484TPM \quad (30)$$ (empirical relationship with TPM concentration used in Duarte et al. (2003))	m^{-1}
Light and temperature limited productivity	$$P_{g(I,T)} = P_{g(I)}.Tlimit \quad (31)$$ where, *Tlimit* – Temperature limitation factor	time^{-1}
Light, temperature and nutrient limited productivity	$$PHYGPP_{ij} = P_{g(I,T,Nut)} =$$ $$P_{g(I,T)} \min\left(\frac{Ncell_{ij}}{k_{Ncell} + Ncell_{ij}}, \frac{Pcell_{ij}}{k_{Pcell} + Pcell_{ij}}\right)$$ (32) where, K_{ncell} – Half saturation constant for growth limited by nitrogen cell quota; K_{pcell} – Half saturation constant for growth limited by phosphorus cell quota.	Time^{-1}
Nitrogen cell quota	$$Ncell_{ij} = \frac{PHYN_{ij}}{PHYC_{ij}} \quad (33)$$ where, *PHYNij* and *PHYCij* represent phytoplankton biomass in nitrogen and carbon units, respectively	mg N mg C^{-1}
Phosphorus cell quota	$$Pcell_{ij} = \frac{PHYP_{ij}}{PHYC_{ij}} \quad (34)$$ where, *PHYPij* represent phytoplankton biomass in phosphorus units	mg P mg C^{-1}
Nitrogen uptake	$$PHYUptakeN_{ij} = V_N.PHYN_{ij} \quad (35)$$	μg N L^{-1} time^{-1}
Phosphorus uptake	$$PHYUptakeP_{ij} = V_P.PHYP_{ij} \quad (36)$$	μg P L^{-1} time^{-1}

Table 7 – Continued - Equations for phytoplankton rate processes. Each rate is multiplied by corresponding carbon, nitrogen or phosphorus stocks to obtain fluxes (see text).

Nitrogen uptake rate (VN)	If $Nmin < PHYN_{ij} < Nmax$ and $PHYN_{ij} / PHYP_{ij} < maxN/P_{ij}$ $$V\,Ammonium = V\max N \frac{NH_{4ij}}{k_{Ammonium} + NH_{4ij}}\left(1 - \frac{Ncell_{ij}}{Nmax}\right)\!(37)$$ $$V\,Nitrate + Nitrite = \max\left(0, V\max_N - V\,Ammonium\right)\cdot$$ $$\frac{NO_{ij}}{k_{Nitrate+Nitrite} + NO_{ij}}\left(1 - \frac{Ncell_{ij}}{Nmax}\right)$$ (38) $$V_N = V\,Ammonium + V\,Nitrate + Nitrite$$ else $$VN = 0, \quad (39)$$ where $Nmin$ – minimal nitrogen cell quota (mg N mg C^{-1}) ; $Nmax$ - maximal nitrogen cell quota (mg N mg C^{-1}) ; $KAmmonium$ – half saturation constant for ammonium uptake (µmol N L^{-1}); $maxN/P_{ij}$ – Maximal cellular nitrogen:phosphorus ratio; V_{maxN}– Maximal uptake rate (d^{-1}); $KNitrate+Nitrite$ – half saturation constant for Nitrate + Nitrite uptake (µmol N L^{-1});	time^{-1}
Phosphorus uptake rate (VP)	If $PHOSmin < PHYP_{ij} < PHOSmax$ and $PHYN_{ij} / PHYP_{ij} > minN/P_{ij}$ $$V_P = V\max P \frac{PO_{4ij}}{k_P + PO_{4ij}}\left(1 - \frac{Pcell_{ij}}{PHOSmax}\right)(40)\ \text{else}$$ $$VP = 0, \text{ where}$$ $PHOSmin$ – minimal phosphous cell quota (mg P mg C^{-1}) ; $PHOSmax$ - maximal phosphous cell quota (mg P mg C^{-1}) ; Kp – half saturation constant for phosphous uptake (µmol P L^{-1}); $minN/P_{ij}$ – Minimal cellular nitrogen:phosphorus ratio; V_{maxP}– Maximal uptake rate (d^{-1});	time^{-1}
Phytoplankton exudation rate of Carbon	$$PHYExud_{ij} = Exud.PHYGPP_{ij}, \text{ where } (41)$$ $Exud$ – Fraction exudated;	time^{-1}

Table 7 – Continued - Equations for phytoplankton rate processes. Each rate is multiplied by corresponding carbon, nitrogen or phosphorus stocks to obtain fluxes (see text).

Phytoplankton respiration rate	$$PHYResp_{ij} = \left(R_0 + R_{dark}.Tlimit.DailyMean\overline{GPP_{ij}} \right).$$ $$\frac{CarbonToOxygen}{ChlorophyllToCarbon}.OxygenMolecularWeight.24 \quad (42)$$ during the night $$PHYResp_{ij} = \left(R_0 + R_{dark}.Tlimit.DLratio.DailyMean\overline{GPP_{ij}} \right).$$ $$\frac{CarbonToOxygen}{ChlorophyllToCarbon}.OxygenMolecularWeight.24 \quad (43)$$ during the day, where $R0$ – Maintenance respiration (mmol O_2 mg Chl^{-1} h^{-1}); R_{dark}– Linear coefficient of increase in biomass-specific dark respiration with gross photosynthesis (dimensionless); DLratio – Ratio between respiration in the light and respiration in the dark (dimensionless); $DailyMean\overline{GPP_{ij}}$ - Daily integrated gross productivity (mmol O_2 mg Chl^{-1} h^{-1}); CarbonToOxygen – Conversion factor between oxygen consumed and carbon produced in respiration (mg C mg $O_2{}^{-1}$); ChlorophyllToCarbon – Conversion factor from chlorophyll to carbon (mg C mg Chl^{-1})	time^{-1}
Temperature limitation factor	$$Tlimit = \exp\left(TempAugRate\left(T_{ij} - T_0 \right) \right) (44)$$ where, TempAugRate – Temperature augmentation rate; T_0 – Reference temperature.	dimensionless
Nitrogen mortality loss	$$PHYMortN_{ij} = PHYMort_{ij}.PHYC_{ij}.Ncell_{ij} \quad (45)$$	μg N l^{-1}time^{-1}
Phosphorus mortality loss	$$PHYMortP_{ij} = PHYMort_{ij}.PHYC_{ij}.Pcell_{ij} \quad (46)$$	μg P l^{-1}time^{-1}
Carbon settling loss rate	$$PHYSet_{ij} = \frac{SettlingSpeed}{Depth_{ij}}, \quad (47)$$ where, *SettlingSpeed* – Fall velocity of phytoplankton cells (m d^{-1}); $Depth_{ij}$ – Depth of layer j in column i (m)	time^{-1}

Table 7 – Continued - Equations for phytoplankton rate processes. Each rate is multiplied by corresponding carbon, nitrogen or phosphorus stocks to obtain fluxes (see text).

Nitrogen settling loss	$PHYSetN_{ij} = SettlingSpeed \cdot \dfrac{PHYN_{ij}}{Depth_{ij}}$ (48)	μg N l^{-1}time^{-1}
Phosphorus settling loss	$PHYSetP_{ij} = SettlingSpeed \cdot \dfrac{PHYP_{ij}}{Depth_{ij}}$ (49)	μg P l^{-1}time^{-1}

Table 8 – Equations for *Enteromorpha sp.* and *Ulva sp.* rate processes. Each rate is multiplied by corresponding dry weight, carbon, nitrogen or phosphorus stocks to obtain fluxes (see text).

Processes	Equations	Units
Steele's equation (Steele, 1962))	$$P_{g(I)} = P_{max} \frac{I_z}{I_{opt}} \exp\left(1 - \frac{I_z}{I_{opt}}\right) \quad (50)$$ where, $Pmax$ – Maximum rate of photosynthesis; I_{opt} – Optimal light intensity for photosynthesis; I_z – Light intensity at depth z;	time^{-1}
Light and temperature limited productivity	$$P_{g(I,T)} = P_{g(I)} \cdot Tlimit \quad (51)$$ where, $Tlimit$ – Temperature limitation factor	time^{-1}
Temperature limitation factor	$$Tlimit = \frac{1}{1 + \exp\left(-\text{TempCoeff}\left(T_{ij} - T_0\right)\right)}$$ (52) where, TempCoeff – Temperature coefficient; T_0 – Reference temperature.	dimensionless
Light, temperature and nutrient limited productivity	$$ENTGPP_{ij} \text{ or } ULVGPP_{ij} = P_{g(I,T,Nut)} =$$ $$P_{g(I,T)} \min\left(\frac{Ncell_{ij} - Nmin}{Nmax - Nmin}, \frac{Pcell_{ij} - PHOSmin}{PHOSmax - PHOSmin}\right)$$ (53) Symbols as before for phytoplankton (cf. – Table 7)	time^{-1}
Enteromorpha nitrogen uptake	$$EntUpDIN_{ij} = V_N \cdot ENT_{ij} \quad (54)$$	g N m^{-2} time^{-1}
Enteromorpha phosphorus uptake	$$EntUpDIN_{ij} = V_P \cdot ENT_{ij} \quad (55)$$	g P m^{-2} time^{-1}

Table 8 – Continued - Equations for *Enteromorpha sp.* and *Ulva sp.* rate processes. Each rate is multiplied by corresponding dry weight, carbon, nitrogen or phosphorus stocks to obtain fluxes (see text).

Ulva nitrogen uptake	$$UlvUpDIN_{ij} = V_N ULV_{ij} \quad (56)$$	g N m⁻² time⁻¹
Ulva phosphorus uptake	$$UlvUpDIN_{ij} = V_P ULV_{ij} \quad (57)$$	g P m⁻² time⁻¹
Nitrogen uptake rate (*VN*)	$$V_N = V \max N \frac{NH_{4ij} + NO_{ij}}{k_{DIN} + NH_{4ij} + NO_{ij}} \max\left(\frac{Nmax - Ncell_{ij}}{Nmax - Nmin}, 0\right) (58)$$ where K_{DIN} – half saturation constant for inorganic nitrogen uptake (μmol N L⁻¹);	time⁻¹
Phosphorus uptake rate (*VP*)	$$V_P = V \max P \frac{PO_{4ij}}{k_P + PO_{4ij}} \max\left(\frac{PHOSmax - Pcell_{ij}}{PHOSmax - PHOSmin}, 0\right)$$ (59)	time⁻¹
Enteromorpha mortality rate	$$ENTMort_{ij} = ENTDeathLoss.ENT_{ij}^{beta} + KTEnt.\frac{MAX\left(OxygenDemand_{ij} - DO_{ij}, 0\right)}{OxygenDemand_{ij}}.ENT_{ij}$$ *KTEnt* – Mortality coefficient for oxygen limitation *OxygenDemandij* – Quantity of oxygen necessary over one time step to support Enteromorpha respiration (only positive when respiration > photosynthesis) (60)	time⁻¹
Ulva mortality rate	$$ULVMort_{ij} = ULVDeathLoss.ULV_{ij}^{beta} + KTUlva.\frac{MAX\left(OxygenDemand_{ij} - DO_{ij}, 0\right)}{OxygenDemand_{ij}}.ULV_{ij}$$ *KTEnt* – Mortality coefficient for oxygen limitation *OxygenDemandij* – Quantity of oxygen necessary over one time step to support Ulva respiration (only positive when respiration > photosynthesis) (61)	time⁻¹

Table 9 - Equations for *Ruditapes decussatus* rate processes.

Processes	Equations	Units
Clearance rate	$$CR = aW^{FC} \quad (62)$$ Where, a – allometric parameter; W – meat dry weight (g); FC – allometric exponent for clearance	L individual^{-1} day^{-1}
Coefficient	$$a = \frac{CR_{st}}{W_{st}^{FC}} \quad (63)$$ Where, $CRst$ – Clearance rate of a standard animal; Wst – meat dry weight of a standar clam (g)	
Clearance rate of a standard clam	$$CR_{st} = \left(-0.003TPM_{ij} + 1.426\right)f(T)f(DO) \quad (64)$$	L individual^{-1} day^{-1}
Temperature limitation	$if\ T_{ij} < 20^{\circ}C$ $$f(T) = 1.0 + 0.045\left(T_{ij} - 20.0\right) \quad (65)$$ $else$ $$f(T) = 1.0 - 0.040\left(T_{ij} - 20.0\right)$$ (66)	Dimensionless
Dissolved oxygen limitation	$if\ DOsat_{ij} > 28\%$ $$f(DO) = 1 \quad (67)$$ $else$ $$f(DO) = 1.0 + 0.06\left(DOsat_{ij} - 28.0\right)$$	Dimensionless
Suspended matter filtration	$$Cons = CR.TPM_{ij}$$	g individual^{-1} day^{-1}
Pseudofaeces production rate	$delta = ThresCons - Cons$ $$PF = PFmax\left(1 - \exp\left(xkp.delta\right)\right) \quad (68) \text{ where,}$$ (69) $ThresCons$ – Threshold filtration rate; $PFmax$ – Pseudofaeces maximal production rate; xkp – Coefficient	Dimensionless

Table 9 – Continued - Equations for *Ruditapes decussatus* rate processes.

Suspended matter ingestion	$Ing = Cons(1-PF)conv$ (70)	g individual^{-1} day^{-1}
Absorption	$A = Ing.AE$ (71) Where, AE – Absorption efficiency	J individual^{-1} day^{-1} (it is converted to/from g individual-1 day-1 assuming an energy contents for the clams of 20000 J g^{-1} (Sobral, (1995))
Absorption efficiency	$AE = AEmax - \dfrac{AP}{OCI}$ Where, $AEmax$ – Maximum absorption efficiency; AP – Empirical coefficient; OCI – Organic contents of ingested food	Dimensionless
Respiration rate	$R = R_{st}\left(\dfrac{W}{W_{st}}\right)^{RC}$ (72) where, R_{st} – respiration of a standar mussel (1 g DW); RC – respiration exponent	J individual^{-1} day^{-1} (it is converted to/from g individual-1 day-1 assuming an energy contents for the clams of 20000 J g^{-1} (Sobral, 1995))
Respiration rate of a standard animal	*If DOsatij < 28% R_{st} = 1.5 else R_{st} = 3.1*	J day^{-1} ind^{-1}

Table 10 – Model parameters and respective values. Most values were calibrated from ranges reported by quoted authors.

Object	Parameter	Value	Reference
Hydrodynamic 2D object	Manning coefficient	$0.03 \text{ s m}^{-1/3}$	Grant and Bacher (2001)
	Eddy diffusivity	$5 \text{ m}^2 \text{ s}^{-1}$	Neves (1985)
Suspended matter object	*CritSpeed*	0.00773 m s-1	Calibrated
	SinkingVelocity	0.4 and 20 m day-1 for POM and TPM, respectively	Calibrated
	Erate	432 g m-2 day-1	Calibrated
Phytoplankton object	*Nmin*	$0.1 \text{ mg N mg C}^{-1}$	Jørgensen et al (1991)
	Nmax	$0.53 \text{ mg N mg C}^{-1}$	"
	KAmmonium	$2.94 \text{ μmol N l}^{-1}$	"
	maxN/Pij	291	"
	VmaxP and VmaxN	1.08 d^{-1}	Cochlan and Harrison (1991)
	KNitrate+Nitrite	30 μmol N l^{-1}	Jørgensen et al (1991)
	PHOSmin	$0.002 \text{ mg P mg C}^{-1}$	"
	PHOSmax	$0.08 \text{ mg P mg C}^{-1}$	"
	minN/Pij	4	"
	Kp	2 μmol P l^{-1}	"
	Pmax	1.1 d^{-1}	"
	Iopt	$850 \text{ μE m}^{-2} \text{ s}^{-1}$	"
	KNcell	$0.028 \text{ mg N mg C}^{-1}$	Calibrated
	KPcell	$0.004 \text{ mg P mg C}^{-1}$	Calibrated
	Exud	0.1	Jørgensen et al (1991)
	$R0$	$0.02 \text{ mmol O}_2 \text{ mg Chl}^{-1} \text{ h}^{-1}$	Langdon (1993)
	R_{dark}	0.3	Calibrated
	DLratio	2	Langdon (1993)
	CarbonToOxygen	$0.3125 \text{ mg C mg O}_2^{-1}$	Vollenweider (1974)
	ChlorophyllToCarbon	$50 \text{ mg C mg Chl}^{-1}$	Jørgensen and Jørgensen (1991)
	TempAugRate	0.069 °C^{-1}	Estimated
	T_0	0°C for photosynthesis and 25°C for respiration	Calibrated
	SettlingSpeed	1 m d^{-1}	Mann and Lazier (1996)
	$PHYMort_{ij}$	0.05 day^{-1}	Jørgensen and Jørgensen (1991)

Table 10 – Continued - Model parameters and respective values. Most values were calibrated from ranges reported by quoted authors

Enteromorpha sp	P_{max}	6.93 mg C g(DW)-1 h-1	Serpa (2004)
	I_{opt}	335 µE m^{-2} s^{-1}	"
	$ENTResp_{ij}$	0.04 mg C g(DW)-1 h-1	"
	T0	0ºC	"
	TempCoeff	1ºC	"
	Nmin	0.01 gN g(DW)-1	"
	Nmax	0.035 gN g(DW)-1	"
	PHOSmin	5 X 10-4 gP g(DW)-1	"
	PHOSmax	4 X 10-3 gP g(DW)-1	"
	$VmaxN$	1.68 mg N g(DW)-1h-1	"
	$VmaxP$	0.23 mg P g(DW)-1h-1	"
	KDIN	0.25 mg L-1	"
	Kp	0.025 mg L-1	"
	ENTDeathLoss	0.00125 h-1	"
	Beta	0.84	Solidoro et al. (1997)
	KTEnt	1	Calibration
Ulva sp.	Pmax	5.14 mg C g(DW)-1 h-1	Serpa (2004)
	Iopt	358 µE m^{-2} s^{-1}	"
	ULVRespij	0.25 mg C g(DW)-1 h-1	"
	T0	0ºC	"
	TempCoeff	1ºC	"
	Nmin	0.01 gN g(DW)-1	"
	Nmax	0.04 gN g(DW)-1	"
	PHOSmin	6 X 10-4 gP g(DW)-1	"
	PHOSmax	3.9 X 10-3 gP g(DW)-1	"
	VmaxN	1 mg N g(DW)-1h-1	"
	VmaxP	0.3 mg P g(DW)-1h-1	"
	KDIN	0.25 mg L-1	"
	Kp	0.025 mg L-1	"
	ULVDeathLoss	0.00125 h-1	"
	beta	0.84	Solidoro et al. (1997)
	KTUlva	1	"
Zostera noltii	Pmax	8X10-4 g O2 mmol C-1 ºC-1 day-1	
(refer Plus et al. (2003) for parameter meaning)	$P_{max}^{0ºC}$	0.0 g O2 mmol C-1 day-1	
	Ikmax	100 Wm-2	Calibration
	Ikmin	35 Wm-2	
	LR	4.5X10-5 g O2 mmol C-1 ºC-1 day-1	
	LR0ºC	5.9X10-4 g O2 mmol C-1 day-1	

Table 10 – Continued - Model parameters and respective values. Most values were calibrated from ranges reported by quoted authors

Ruditapes decussatus	*Wst*	0.3 g	Sobral (1995)
	FC	0.7	"
	ThresCons	0.0 g individual-1 day-1	Calibration
	xkp	0.8	"
	PFmax	1.0	"
	AP	0.07	"
	AEmax	0.85	"
	m	4X10-3 day-1	Falcão et al. (2000)
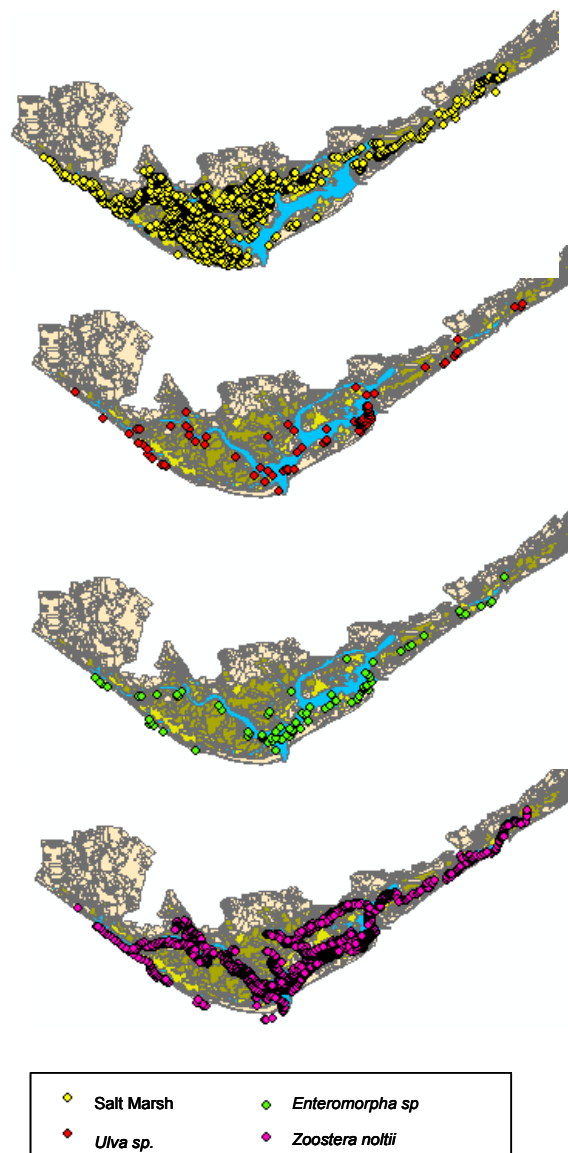
Fig. 2 – GIS images showing Ria Formosa benthic primary producers considered in this work – Salt Marshes, *Ulva sp.*, *Enteromorpha sp* and *Zostera noltti*
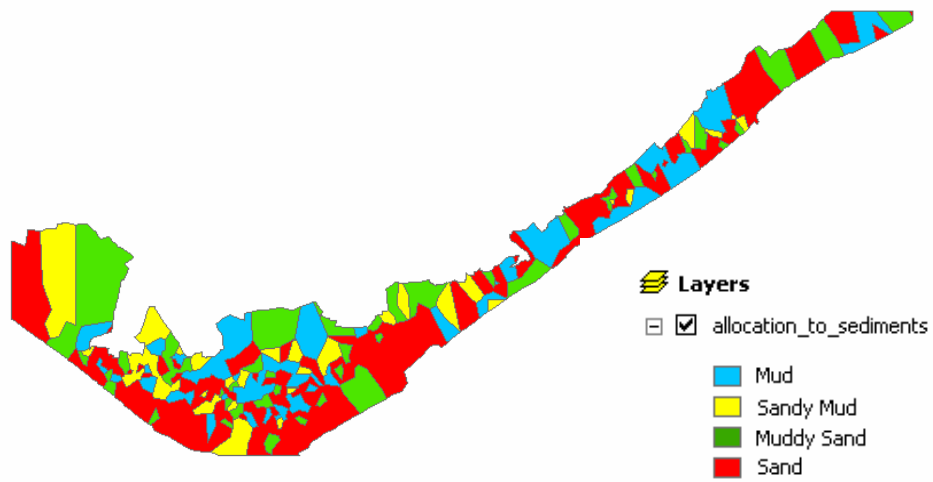
Fig. 3 – GIS image showing sediments type distribution in Ria Formosa.
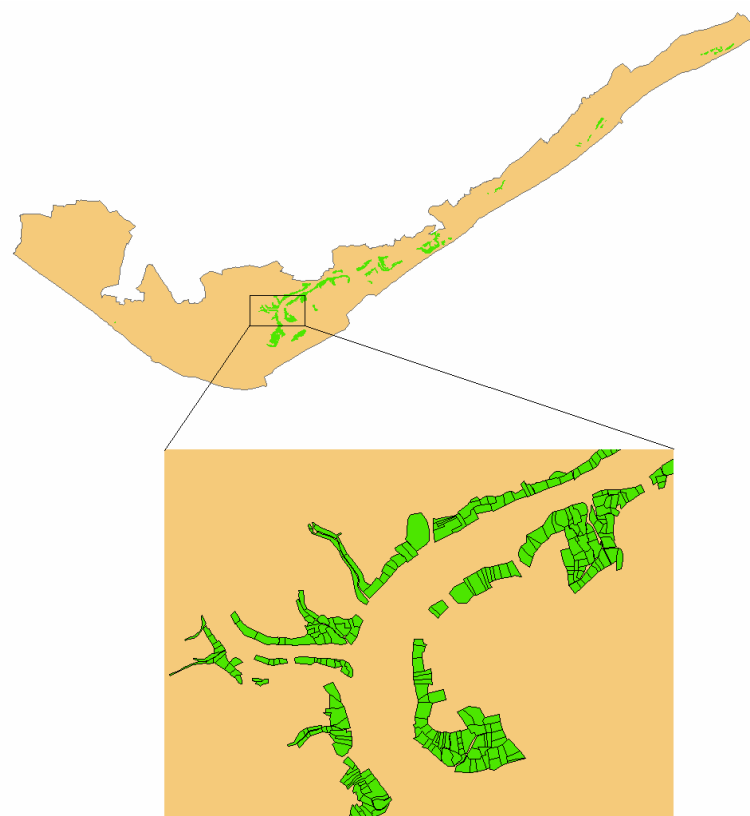
Fig. 4 – Ria Formosa shellfish farming areas.
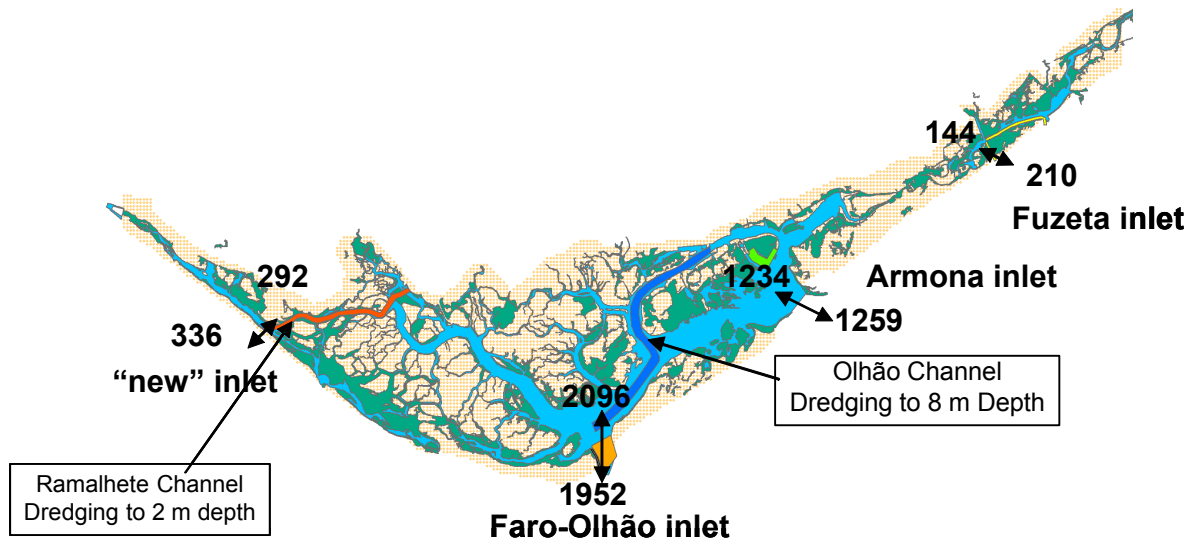
Fig. 5 – Scenario localization regarding changes in lagoon bathymetry. In the Ramalhete scenarios, average depth is increased by c.a. 0.5 m. In the Olhão channel, depth is increased two fold. Also shown Ria Formosa inlets and average inflows and outflows in ($m^3 \ s^{-1}$).

Results and discussion

The first part of this section (Model testing) synthesises some comparisons between observed and simulated data (under the standard simulation). The second part deals with scenario analysis, where results obtained with several simulations are compared to those of the standard simulation.

Model testing

Comparisons between observed and predicted values in the Standard simulation (cf. – Methodology – Model testing) are shown in Figs. 6 – 11 for nitrate, ammonia, phosphate and water temperature. Observations were made during the ebb and during the flood for each sampling occasion. Nutrient flood values are lower than ebb values and closer to the sea boundary conditions, except for nitrate in some occasions. This is also the case for simulated data, as can be seen for nitrate in Fig. 6, shown together with water depth.

The small number of observations prevents any powerful statistical test to quantify model performance. Furthermore, data is available only for a small number of stations located not very distant from one another (c.a. 500 – 1000 m) and for a small number of variables. However, in most situations, the ranges predicted by the model are within those observed, with a poorer performance for ammonium and nitrate - slightly overestimated by the model. Comparisons were also made for water column chlorophyll, sediment pore water nutrient and oxygen concentrations and sediment carbon, nitrogen and phosphorus contents. However, available data for these variables were obtained in different years than water quality data shown in Figs. 6 – 11. Therefore, these comparisons were just to make sure that model predictions remained within the range of observations, which was the case.

The model is able to predict *R. decussatus* individual weight well within the range of values observed in Ria Formosa (Fig. 12). Clams grow from an initial weight of c.a. 12 g to a weight ranging between 0.2 and 0.4 g of meat dry weight.
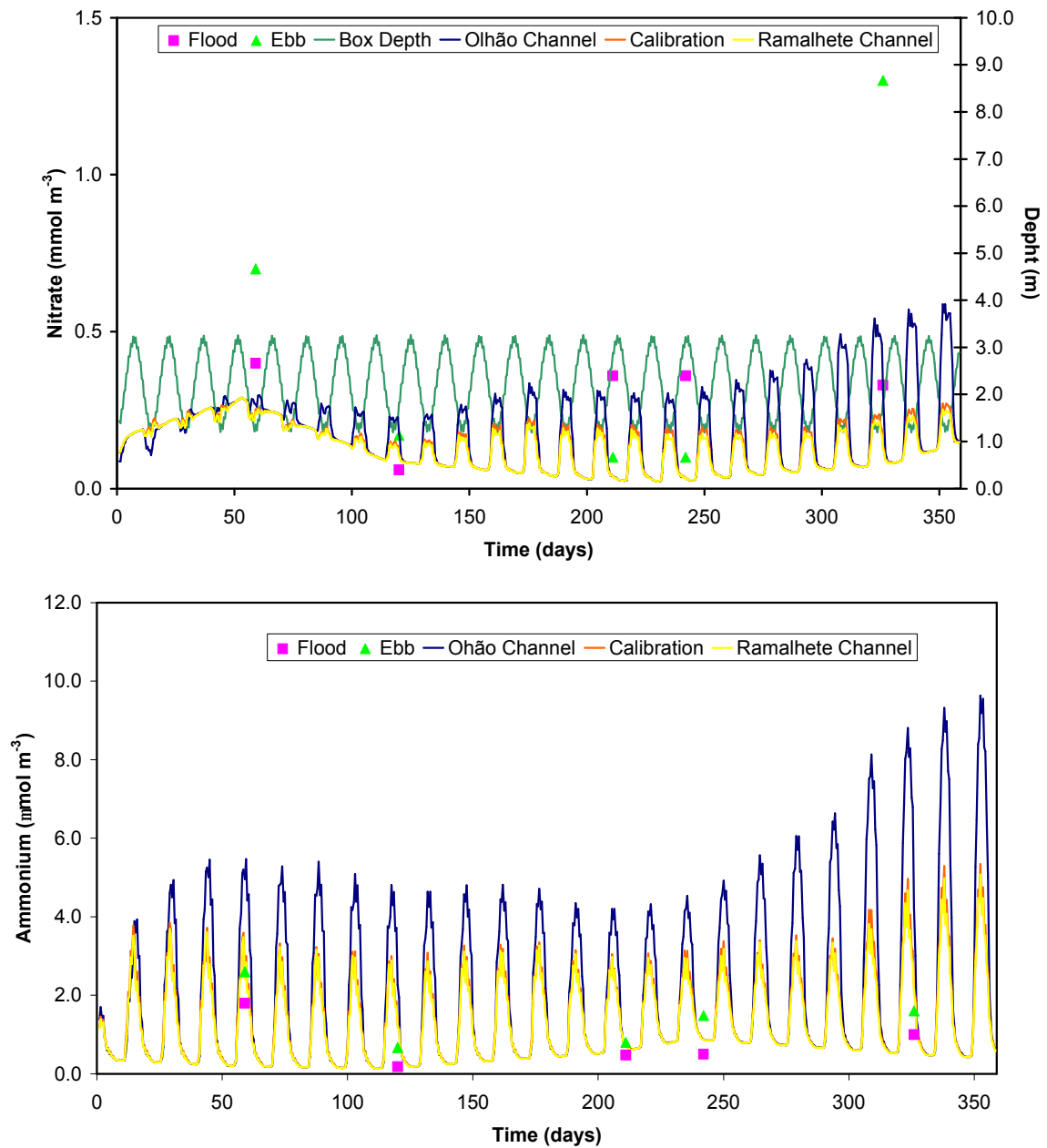
Fig. 6 – Simulated and observed nitrate (upper chart) and ammonia (lower chart) at station RA. Also shown simulated box depth to emphasize the opposite trends between concentration and water depth (upper chart) and the results obtained with other scenarios (see text).
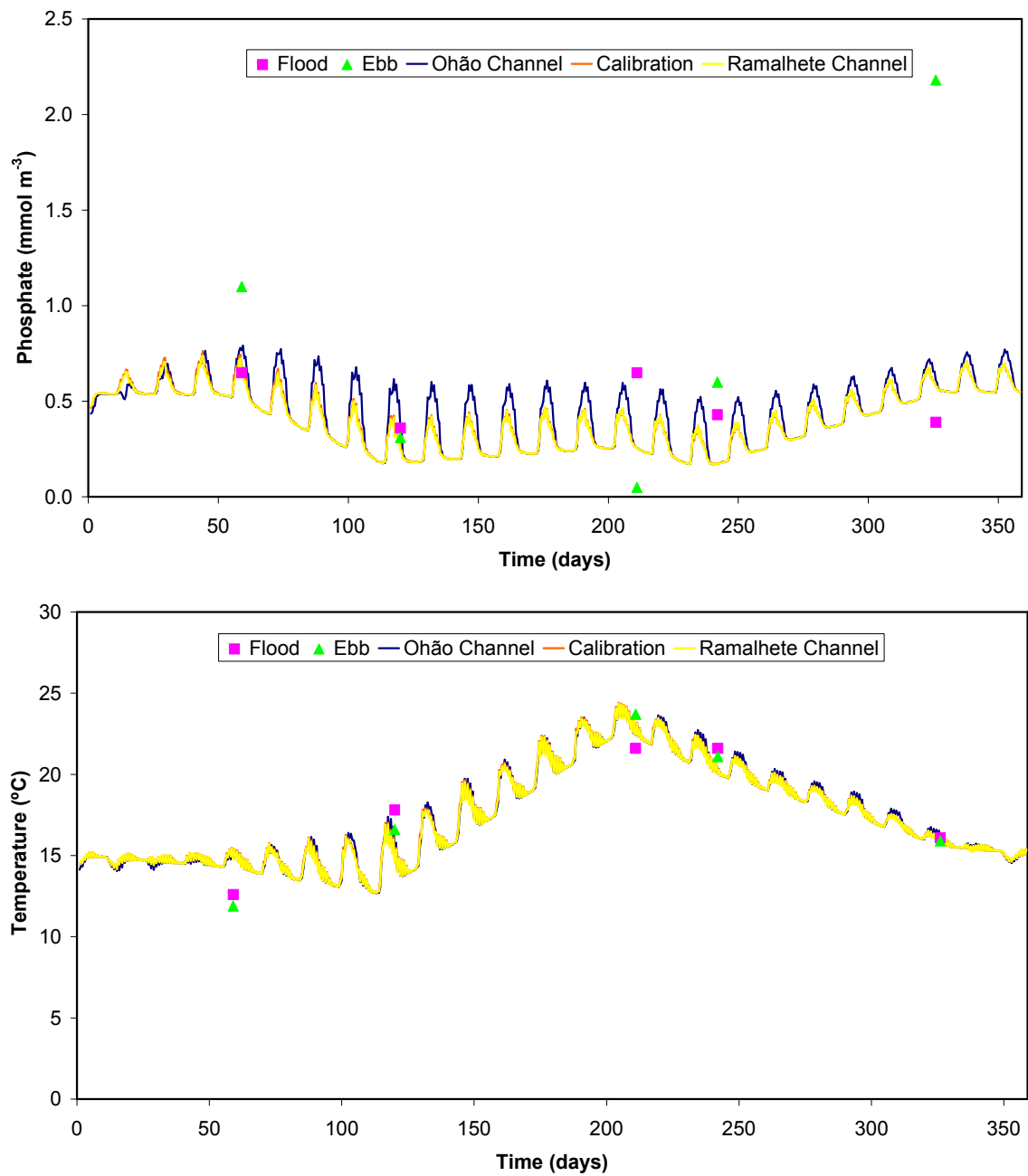
Fig. 7 – Simulated and observed phosphate (upper chart) and water temperature (lower chart) at station RA.
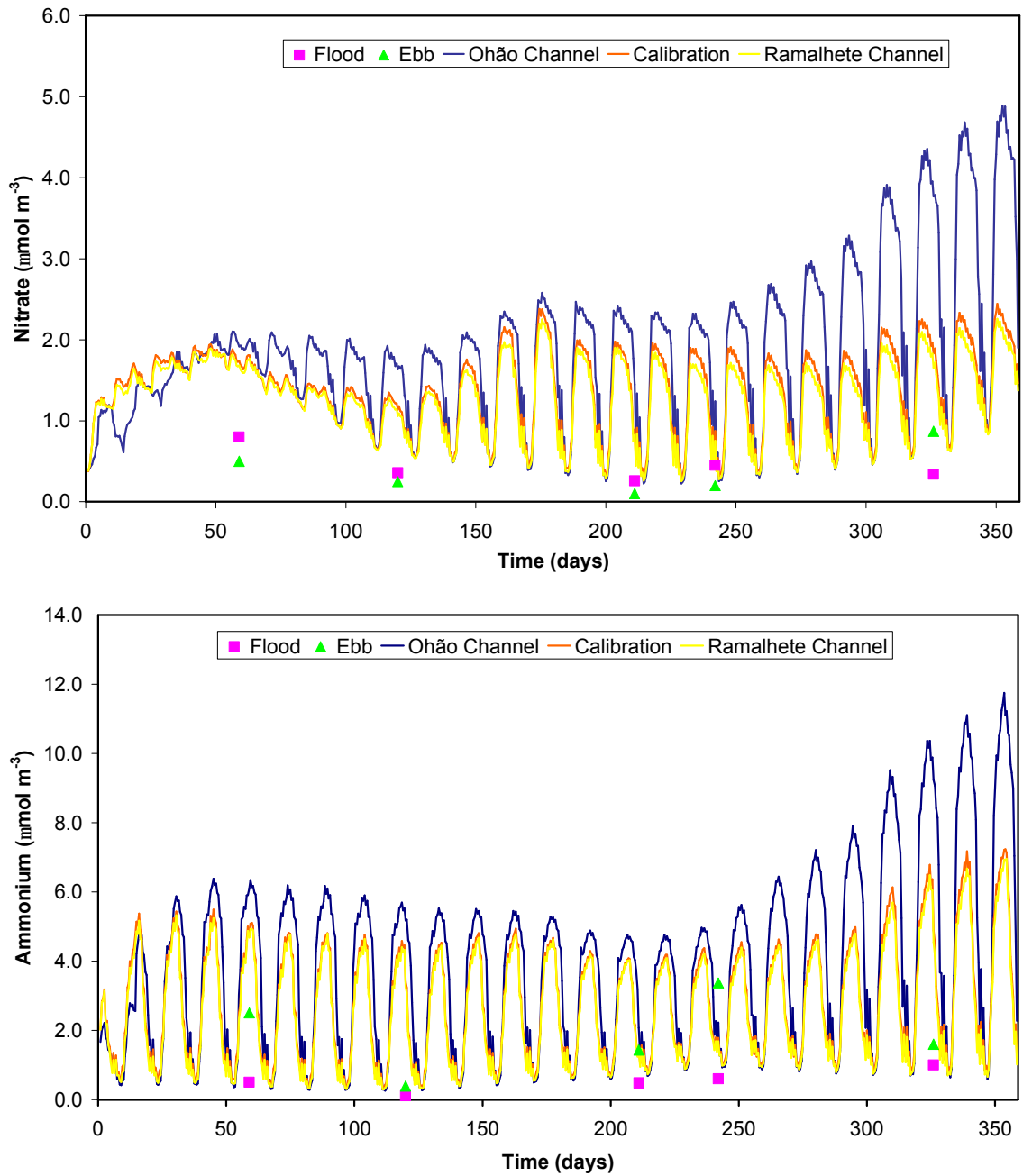
Fig. 8 – Simulated and observed nitrate (upper chart) and ammonia (lower chart) at station RB.
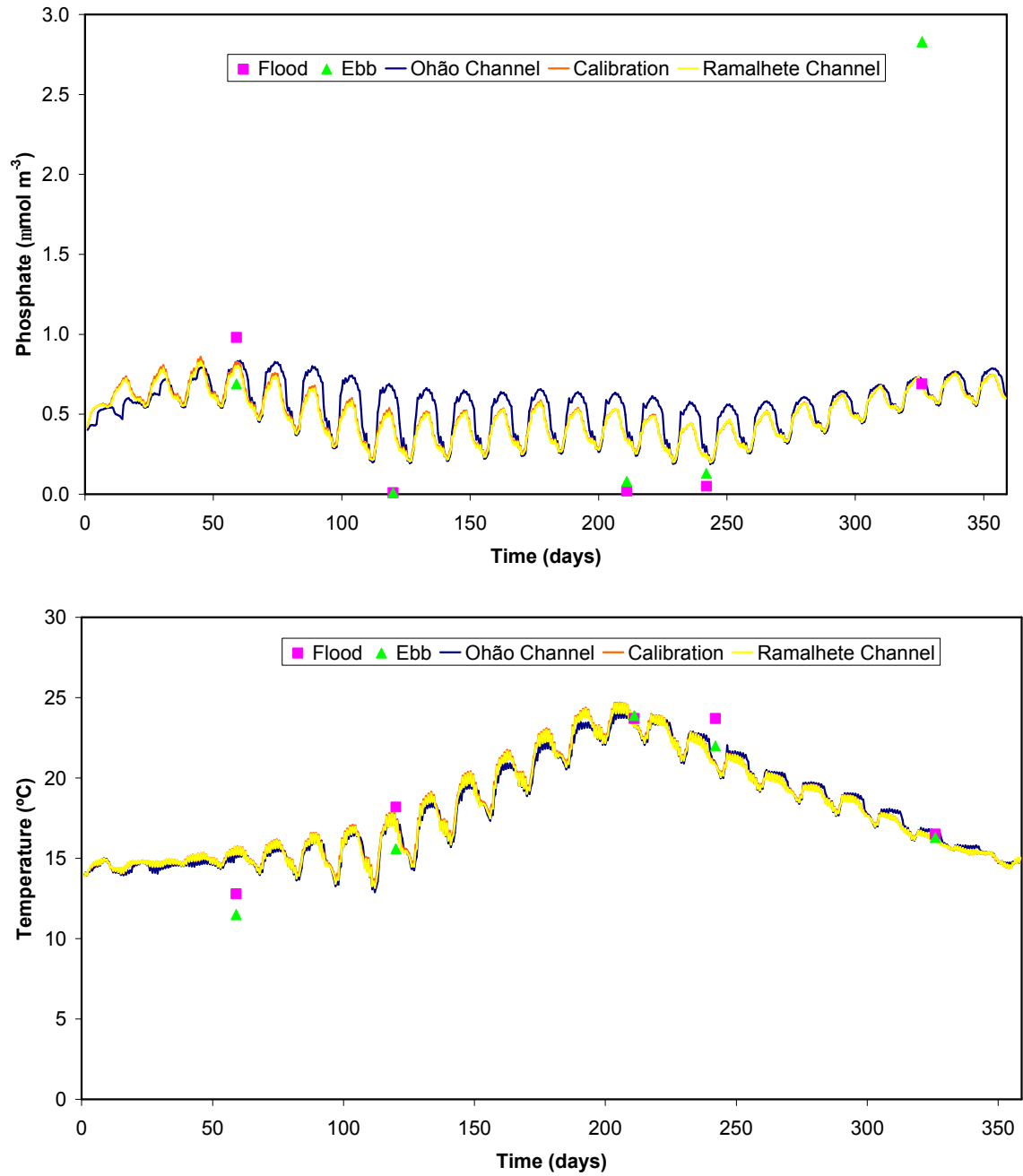
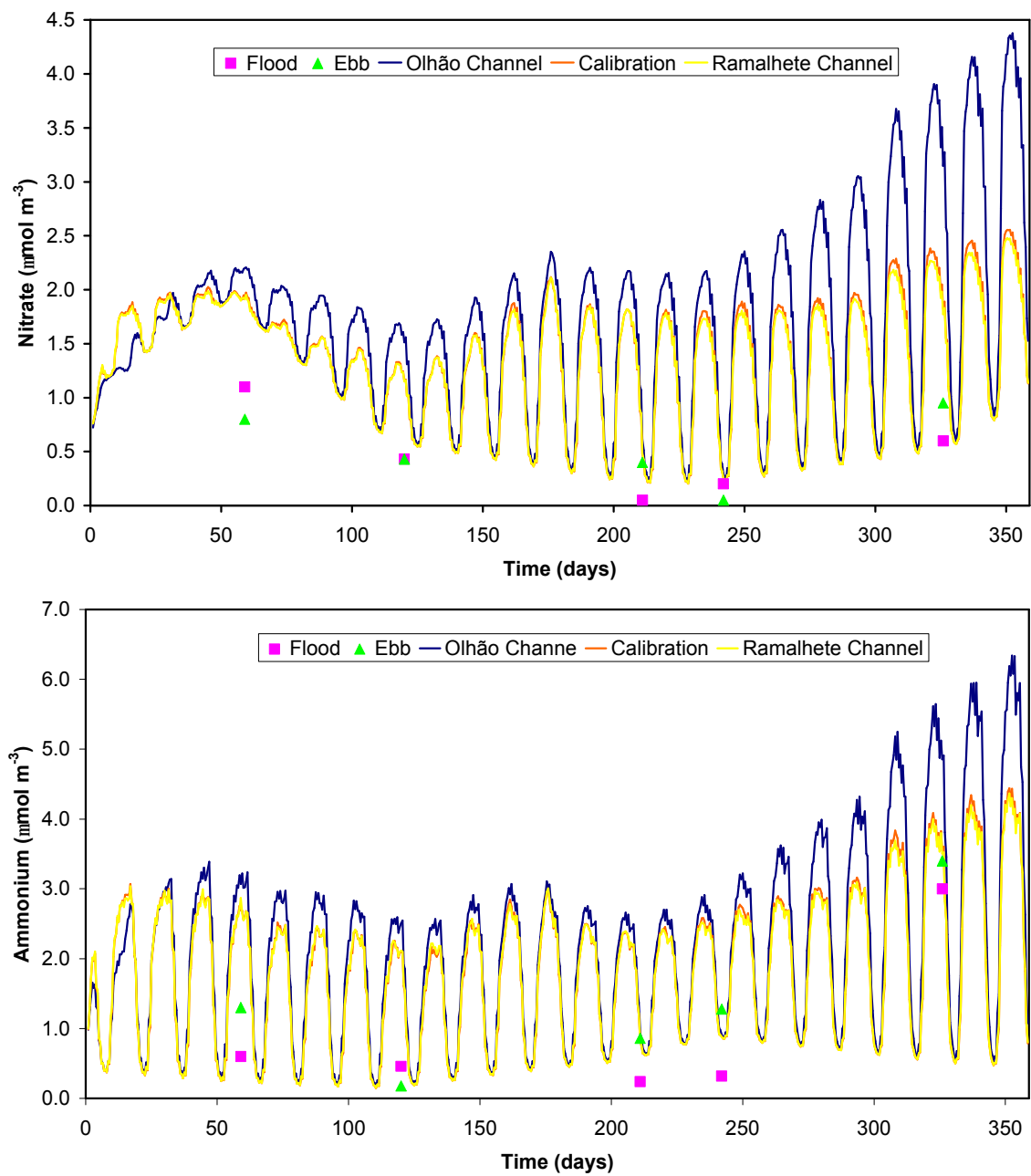Fig. 9 – Simulated and observed phosphate (upper chart) and water temperature (lower chart) at station RB.

Fig. 10 – Simulated and observed nitrate (upper chart) and ammonia (lower chart) at station RC
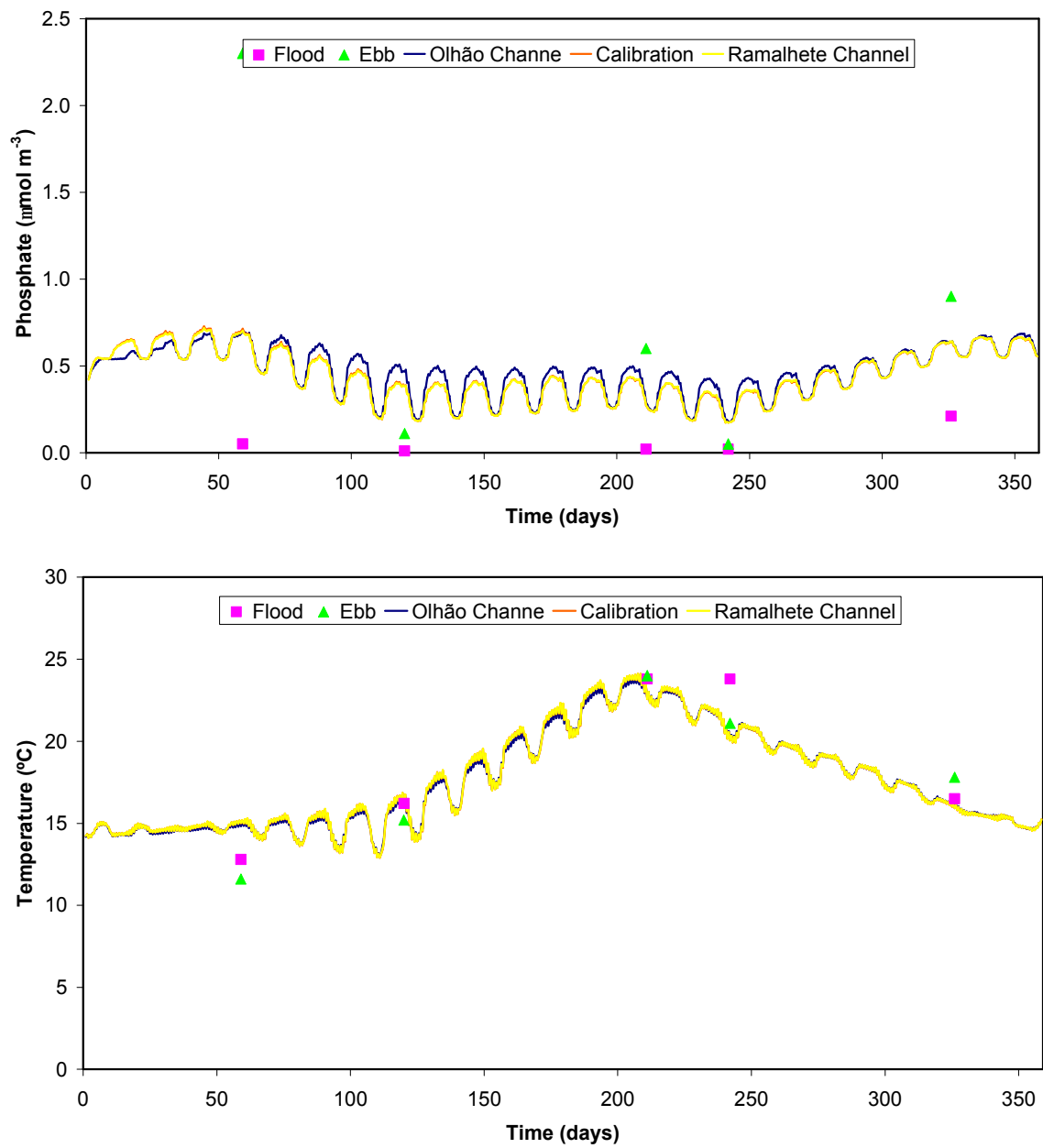
Fig. 11 – Simulated and observed phosphate (upper chart) and water temperature (lower chart) at station RC.
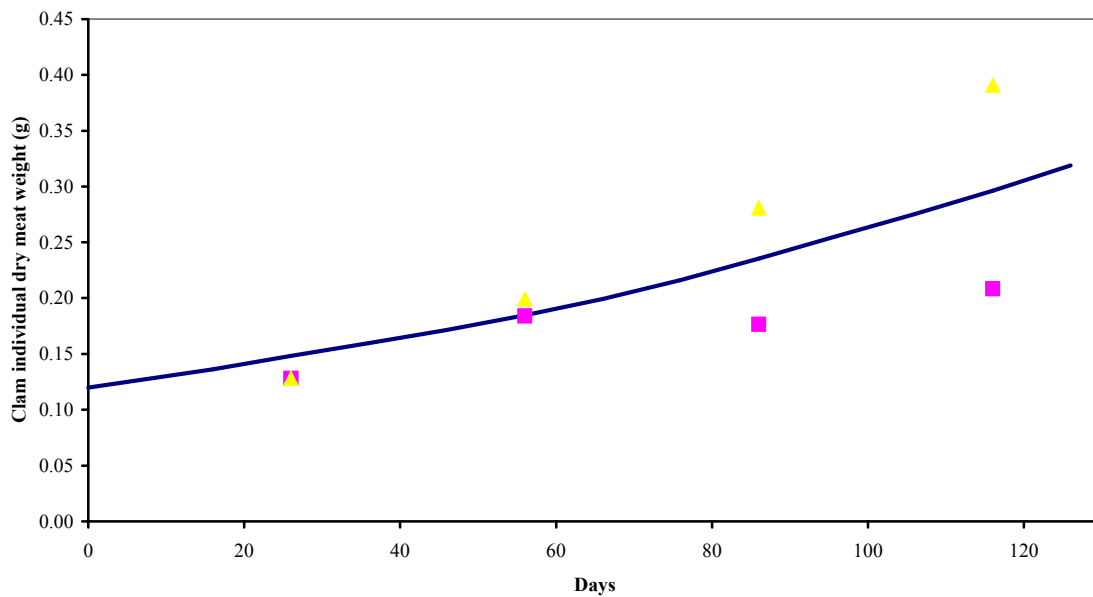
Fig. 12 – Predicted (line) and observed *R. decussatus* weight at two different points (triangles and squares), over a period of c.a. half a year. Observed data was taken from Falcão et al. (2000).

Scenario analysis

Tables 11 and 12 present a comparison between the Standard simulation and the Olhão and Ramalhete Channel scenarios (cf. – Methodology – Scenario analysis), regarding water column and sediment variables, averaged over a period of one year. Obtained results suggest that dredging the mentioned channels do not contribute to an improvement on water quality. In fact, in the case of the Olhão scenario, two variables instead of one fall into the category "Discrete". Regarding sediment quality, model results suggest an improvement, in the case of the Ramalhete scenario, with all variables falling into the category "Very Good". In previous works (Duarte et al., 2006; Duarte et al., in press) it was shown that dredging the Olhão and the Ramalhete Channels leads to an increase in water residence time. Perhaps this increase may explain partly the apparent worsening in water quality under the Olhão scenario.

Table 13 synthesises results obtained for the simulations with different bivalve densities (cf. – Methodology – Scenario analysis). Results related to water quality were integrated in time and space, over clam rearing areas (Fig. 4) and suggest a clear worsening on water quality with increasing bivalve densities, especially concerning nitrate and ammonium concentrations, with ammonium values falling into category "bad", under the largest density – 3 kg (FW) m^{-2}. The ammonium increase is a result of bivalve excretion and the nitrate increase a result of ammonium mineralization. When results are integrated over the entire model domain (not shown), water quality remains in categories "Very good" and "Good". Increasing bivalve densities did not produce any worsening of sediment quality.

The relationship between seeding density and bivalve final biomass (corresponding to marketable production), net gain in biomass and individual weight is shown in Fig. 13. From obtained results, it is apparent that final biomass could be increased by increasing initial biomass standing stock. However, this increase would be at the expenses of the larger initial standing stock, with an important reduction on bivalve growth and individual weight. Furthermore, net gain in biomass (the difference between final and initial biomass) under the half and the standard density scenarios are approximately the same, in spite of the two-fold initial biomass investment under the latter. Under larger cultivation densities, final biomasses may be lower than initial ones.

From obtained results, it may be argued that Ria Formosa rearing areas are probably being exploited close to their carrying capacity. In fact, considering that the clearance rate of a clam weighing 0.12 g of meat dry weight (weight at the beginning of the simulations) is approximately 0.7 L h^{-1} and that bivalve cultivation density is around 450 individuals m-2, it may be estimated a daily water pumping rate of over 80000 m^3 at the area corresponding to a model grid cell (10000 m^2). This implies that, on average, clams may pump all the water, overlaying cultivation areas, in c.a. 6 hours. Considering that water residence time over the cultivation areas (estimated from the ratio between average volume of corresponding model grid cells and their average water inflows/outflows) is c.a. 18 hours, it is apparent that clams may be food limited, unless compensated by local production, such as phytoplankton growth or suspended detritus pathways from macrophyte and macroalgae decomposition.

Clam individual weight isolines are shown in Fig. 14, at the beginning of the standard simulation, after 50 and 100 days. It is apparent that growth is far from uniform. This is expected, considering the environmental variability of the lagoon in terms of current speeds and organic suspended matter transport – the clam food source. These results may be helpful in identifying the relative quality of rearing areas and those where carrying capacity have been exceeded to a larger degree. Considering the results discussed in the previous paragraphs, it seems advisable to keep clam biomass standing stocks at present levels (standard scenario) or even to decrease them. This could lead to an improvement in water quality and also on bivalve growth. More growth would probably reduce mass summer mortalities, frequently reported by farmers. Furthermore, any increase in clam production should be at the expenses of increasing rearing areas and not though biomass density increases in current cultivation zones.

Table 11 – Water quality assessment for the standard simulation, the Olhão Channel and the Ramalhete Channel scenarios, following the IFREMER classification scheme (cf. – Methodology – Scenario analysis). Average values shown for each variable, integrated for a period of one year, for the entire model domain (see text). All values fall into categories "Very good", "Good" and "Discrete". Remaining categories are "Sufficient" and "Bad" (Austoni *et al*., 2004).

			Very good	Good	Discrete
Standard simulation	O_2	Δ % Sat.	6.93		
	PO_4^{3-}	µM			1.07
	NO_2 -N	µM	0.04		
	NO_3 -N	µM		7.34	
	NH_4 -N	µM		9.70	
	Chl-a	µgl^{-1}	0.78		
Olhão Channel	O_2	Δ % Sat.	6.49		
	PO_4^{3-}	µM			1.15
	NO_2 -N	µM	0.04		
	NO_3 -N	µM		9.19	
	NH_4 -N	µM			10.28
	Chl-a	µgl^{-1}	0.74		
Ramalhete Channel	O_2	Δ % Sat.	6.98		
	PO_4^{3-}	µM			1.14
	NO_2 -N	µM	0.06		
	NO_3 -N	µM		9.11	
	NH_4 -N	µM		9.85	
	Chl-a	µgl^{-1}	0.77		

Table 12 – Sediment quality assessment for the standard simulation, the Olhão Channel and the Ramalhete Channel scenarios, following the IFREMER classification scheme (cf. – Methodology – Scenario analysis). Average values shown for each variable (OM – Organic matter; TN – Total nitrogen; TP – Total phosphorus), integrated for a period of one year, for the entire model domain (Fig. 1) (see text). All values fall into categories "Very good" and "Good". Remaining categories are "Discrete", "Sufficient" and "Bad" (Austoni *et al.*, 2004).

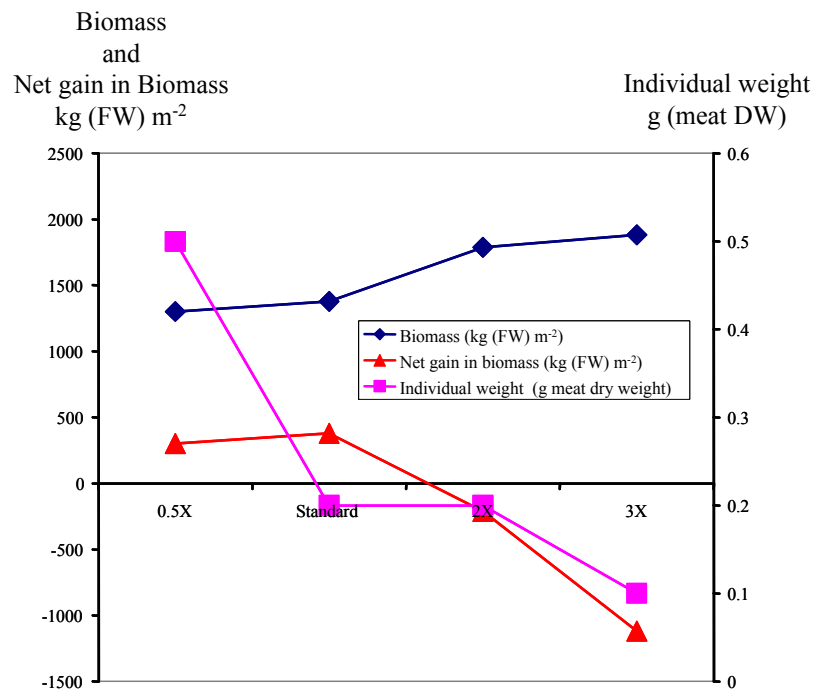|			Very Good	Good
Standard simulation	OM	%	1.03	
	TN	g Kg^{-1} (DW)		1.46
	TP	mg Kg^{-1} (DW)	240.15	
Olhão Channel	OM	%	1.07	
	TN	g Kg^{-1} (DW)		1.06
	TP	mg Kg^{-1} (DW)	204.37	
Ramalhete Channel	OM	%	1.06	
	TN	g Kg^{-1} (DW)	0.97	
	TP	mg Kg^{-1} (DW)	194.47	

Fig. 13 – *R. decussatus* final average biomass, net gain in biomass (Fresh weight - FW) and individual weigh (meat dry weight – DW), under different seeding densities – half, standard, double and triple density, corresponding to initial biomasses of 0.5, 1, 2 and 3 kg (FW) m^{-2}, respectively (cf. –Methodology – *Scenario Analysis*).

Table 13 – Water quality assessment for the simulations with variable bivalve densities, following the IFREMER classification scheme (cf. – Methodology – Scenario analysis). Average values shown for each variable, integrated for a period of half a year and for the rearing areas (Fig. 4) (see text).

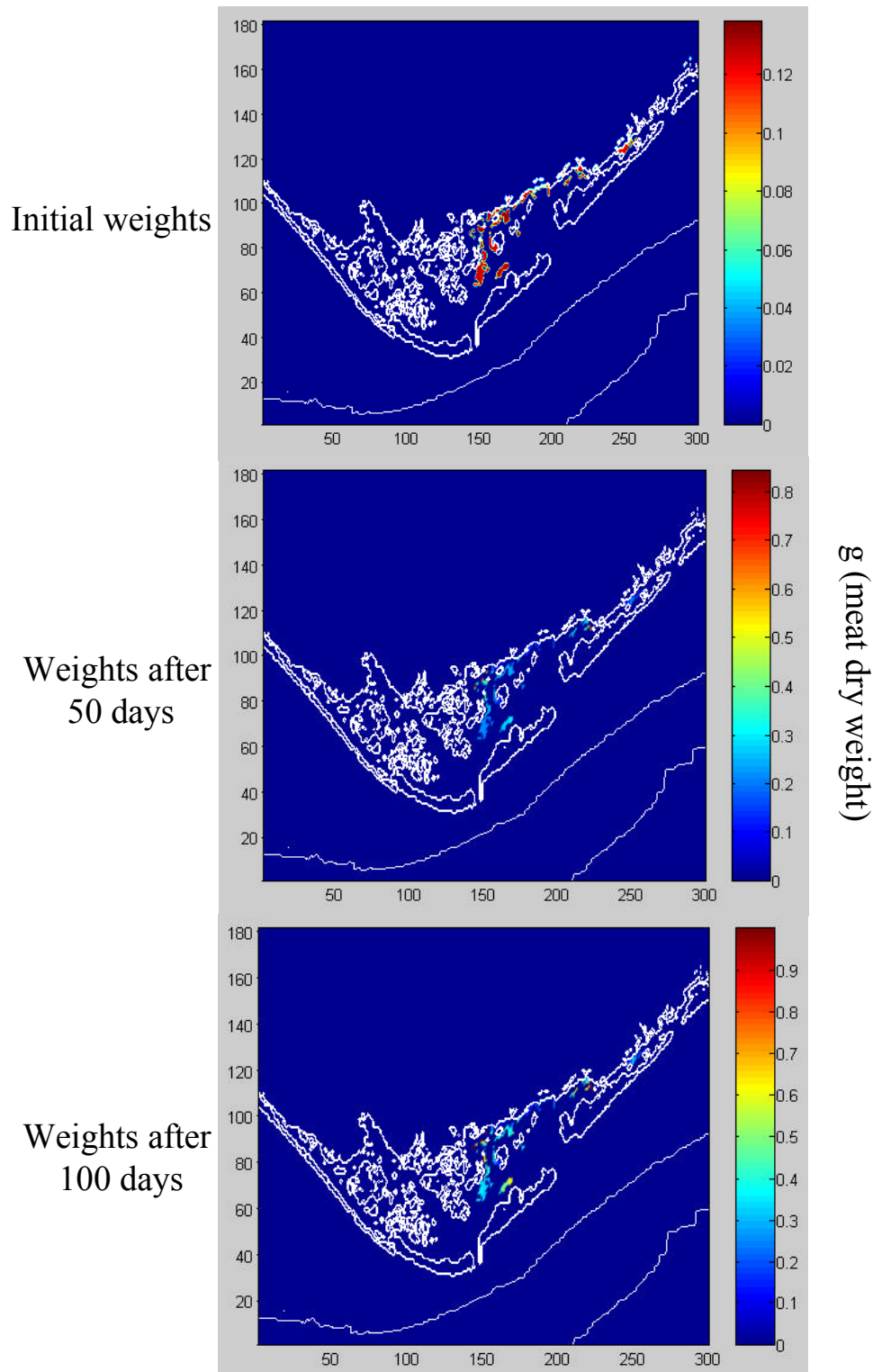|			Very good	Good	Discrete	Sufficient	Bad
1/2 X normal density 0.5 kg (FW) m^{-2}	O_2	Δ % Sat.	2.60				
	PO_4^{3-}	μM		0.76			
	NO_2 -N	μM	0.01				
	NO_3 -N	μM		8.22			
	NH_4 -N	μM		7.85			
	Chl-a	$\mu g L^{-1}$	0.76				
Normal density 1 kg (FW) m^{-2} (Standard simulation)	O_2	Δ % Sat.	2.49				
	PO_4^{3-}	μM		0.76			
	NO_2 -N	μM	0.01				
	NO_3 -N	μM			14.41		
	NH_4 -N	μM			11.87		
	Chl-a	$\mu g L^{-1}$	0.61				
2X normal density 2 kg (FW) m^{-2}	O_2	Δ % Sat.	1.79				
	PO_4^{3-}	μM		0.76			
	NO_2 -N	μM	0.01				
	NO_3 -N	μM				24.11	
	NH_4 -N	μM				21.19	
	Chl-a	$\mu g L^{-1}$	0.53				
3X normal density 3 kg (FW) m^{-2}	O_2	Δ % Sat.	2.19				
	PO_4^{3-}	μM		0.75			
	NO_2 -N	μM	0.01				
	NO_3 -N	μM				28.95	
	NH_4 -N	μM					34.73
	Chl-a	$\mu g L^{-1}$	0.54				

Fig. 14 – *R. decussatus* weight isolines predicted by the model.

Conclusions

From the results presented and discussed, some conclusions may be drawn. It is apparent that changes in lagoon bathymetry analysed so far, do not have an improving effect on water quality. The opposite is apparent concerning sediment quality for one of the scenarios analysed. Clam production may be above carrying capacity of rearing areas. Reducing clam cultivation density should have a positive effect on water quality and clam growth. It does

not seem advisable to increase density in present rearing areas. Therefore, if any clam production increase is to be attempted it should be though increasing rearing areas. These and other aspects will be analysed in upcoming works.

Acknowledgements

References

Austoni M, Viaroli P, Giodani G, Zaldíval JM, 2004. Intercomparison among the test sites of the DITTY project using the IFREMER classification scheme for coastal lagoons. Institute for Environment and Sustainability, Island and Waters Unit. Available at http://www.dittyproject.org/Reports.asp.

Borland 1988. Turbo Pascal. Object-oriented programming guide. Borland International, Inc., 124 pp.

Brock TD 1981. Calculating solar radiation for ecological studies. *Ecological Modelling* **14** 1 - 9.

Burns LA 2000. Exposure analysis modelling system (EXAMS): User manual and system documentation. U.S. Environmental Protection Agency.

Chapelle A 1995. A preliminary model of nutrient cycling in sediments of a Mediterranean lagoon. *Ecological Modelling* **80**: 131-147.

Chapelle A, Ménesguen A, Deslous-Paoli JM, Souchu P, Mazouni N, Vaquer A, Millet B, 2000. Modelling nitrogen, primary production and oxygen in a Mediterranean lagoon. Impact of oysters farming and inputs from the watershed. *Ecological Modelling* **127**: 161-181.

Cochlan WP, Harrison PJ 1991. Uptake of nitrate, ammonium, and urea by nitrogen-starved cultures of Micromonas pusilla (Prasinophyceae): transient esponses. *Journal of Phycology* **67**: 673-679.

Costanza R, Andrade F (eds.) 1998. Ecological economics and sustainable governance of the oceans. FLAD, IMAR, LPN.

Duarte P, Meneses R, Hawkins AJS, Zhu M, Fang J, Grant J 2003. Mathematical modelling to assess the carrying capacity for multi-species culture within coastal water. *Ecological Modelling* **168**: 109-143.

Duarte P, Azevedo B, Pereira A 2005. Hydrodynamic Modelling of Ria Formosa (South Coast of Portugal) with EcoDynamo. DITTY report. Available at http://www.dittyproject.org/Reports.asp.

Duarte P, Azevedo B, Pereira A, Falcão M, Serpa D, Reia J 2006. Scenario Analysis in Ria Formosa with EcoDynamo. Part I. DITTY report. Available at http://www.dittyproject.org/Reports.asp.

Duarte P, Azevedo B, Guerreiro M, Ribeiro C, Bandeira R, Pereira A, Falcão M, Serpa D, Reia J, in press. Biogeochemical Modelling of Ria Formosa (South Portugal). *Hydrobiology.*

Ducobu H, Huisman J, Jonker, RR, Mur LR, 1998. Competition between a Prochlorophyte and a Cyanobacterium under various phosphorus regimes: comparison with the Droop model. *Journal of Phycology* **34**: 467-476.

EC (European Commission) 2000. Directive 2000/60/EC of the European Parliament and of the Council of 23 October 2003 establishing a framework for Community action in the field of water policy. *Official Journal of the European Communities* L32, 22.12.2000, p.1.

Falcão MM 1996. Dinâmica dos nutrientes na Ria Formosa: efeitos da interacção da laguna com as suas interfaces na reciclagem do azoto, fósforo e sílica. PhD, University of Algarve.

Falcão M 1997. Dinâmica de nutrientes na Ria Formosa: efeitos da interacção da laguna com as suas interfaces na reciclagem do azoto, fósforo e sílica. PhD Thesis, Universidade do Algarve, 223 p.

Falcão MM, Duarte P, Matias D, Joaquim S, Fontes T, Meneses R 2000. Gestão do cultivo de bivalves na Ria Formosa com recurso à modelação matemática. Instituto de Investigação das Pescas e do Mar.

Falcão M, Fonseca L, Serpa D, Matias D, Joaquim S, Duarte P, Pereira A, Martins C, Guerreiro MJ 2003. Synthesis report. Available at http://www.dittyproject.org/Reports.asp.

Ferreira J, Duarte P, Ball B 1998. Trophic capacity of Carlingford Lough for aquaculture - analysis by ecological modelling. *Aquatic Ecology* **31 (4)**: 361 – 379.

Grant J, Bacher C 2001. A numerical model of flow modification induced by suspended aquaculture in a Chinese Bay. Can. *Journal of Fisheries and Aquatic Sciences* **58**: 1 - 9.

Guerreiro MJ, Martins C 2005. Calibration of SWAT Model: Ria Formosa Basin (South Coast of Portugal). DITTY report. Available at http://www.dittyproject.org/Reports.asp.

Hawkins AJS, Bayne BL, Bougrier S, Héral M, Iglesias JIP, Navaro E, Smith RFM,. Urrutia MB 1998. Some general relationships in comparing the feeding physiology of suspension-feeding bivalve molluscs. *Journal of Experimental Marine Biology and Ecology* **219**: 87-103.

HPS 1997. An introduction to systems thinking. Stella® software. High Performances Systems.

Honey M 1999. Ecotourism and sustainable development: Who owns paradise? Island Press.

INAG (Instituto da Água) 2005. Relatório síntese sobre a caracterização das regiões hidrográficas prevista na Directiva-Quadro da água. Instituto da Água, Ministério do Ambiente, do Ordenamento do Território e do Desenvolvimento Regional.

Jørgensen SE, Bendoricchio G 2001. Fundamentals of ecological modelling. Developments in Ecological Modelling 21. Elsevier, Amsterdam, 530 p.

Jørgensen SE, Nielsen S, Jørgensen L 1991. Handbook of Ecological Parameters and Ecotoxicology. Elsevier, Amsterdam, 1263 p.

Knauss, J.A. 1997. Introduction to physical oceanography. Prentice-Hall.

Hoijman SLM 2003. Dynamic energy and mass budgets in biological systems. Cambridge University Press.

Langdon C 1993. The significance of respiration in production measurements based on oxygen. ICES mar. Sci. Symp. **197**: 69-78.

MAOT (Ministério do Ambiente e do Ordenamento do Território) 2000. Plano de Bacia Hidrográfica das Ribeiras do Algarve – Caracterização Geral da Bacia Hidrográfica, 1ª Fase – Análise e Diagnóstico da Situação de Referência, Vol. III.

Mann KH, Lazier JRM 1996. Dynamics of marine ecosystems. Blackwell Science.

Neves RJJ 1985. Étude expérimentale et modélisation mathématique des circulations transitoire et rédiduelle dans l'estuaire du Sado. Ph.D. Thesis, Université de Liège.

Park K, Jung H-S, Kim H-S, Ahn S-M 2003. Estuarine and coastal water quality modelling: Concept and a case study in Korea. In: Yu and Bermas (eds.) Determining Environmental Carrying capacity of coastal and marine areas: Progress, constraints, and future options, GEF/UNDP/IMO, PEMSEA: 98 – 114.

Parsons TR, Takahashi M, Hargrave B, 1984. Biological oceanographic processes. 3rd. Edition. Pergamon Press.

Pereira A, Duarte P 2005 EcoDynamo Ecological Dynamics Model Application. University Fernando Pessoa. DITTY report. Available at http://www.dittyproject.org/Reports.asp.

Pereira A, Duarte P, Norro A 2006. Different modelling tools of aquatic ecosystems: A proposal

for a unified approach. *Ecological Informatics* **1**: 407-421.

Plus M, Chapelle A, Ménesguen A, Deslous-Paoli J-M, Auby I 2003. Modelling seasonal dynamics of biomasses and nitrogen contents in a seagrass meadow (*Zostera noltti* Hornem.): application to the Thau lagoon (French Mediterranean coast). *Ecological Modelling* **161**: 213-238.

Plus M, Jeunesse I, Bouraouic F, Zaldívar J-M, Chapelle A, Lazure P 2006. Modelling water discharges and nutrient inputs into a Mediterranean lagoon. Impact on the primary production. *Ecological Modelling* **193**: 69-89.

Portela LI, Neves R 1994. Modelling temperature distribution in the shallow Tejo estuary. In: Tsakiris and Santos (eds.) Advances in Water Resources Technology and Management, Balkema, Rotterdam, pp. 457 - 463.

Raillard O, Deslous-Paoli J-M, Héral M,. Razet D 1993. Modélisation du comportement nutritionnel et de la croissance de l'huître japonaise Crassostrea gigas." *Oceanologica Acta* **16**: 73-82.

Raillard O, Ménesguen A 1994. An ecosystem box model for estimating the carrying capacity of a macrotidal shellfish system. *Marine Ecology Progress Series* **115**: 117-130.

Rodrigues A, Carvalho A, Reia J, Azevedo B, Martins C, Duarte P, Serpa D, Falcão M 2005. A geographical information system for Ria Formosa (South coast of Portugal). DITTY report. Available at http://www.dittyproject.org/Reports.asp.

Serpa D 2004. Macroalgal (Enteromorpha spp. and Ulva spp.) primary productivity in the Ria Formosa lagoon. Master thesis, Faculty of Science and Technology, New University of Lisbon.

Sobral MPO 1995. Ecophysiology of Ruditapes decussatus L. (Bivalvia, Veneridae). PHD thesis, Universidade Nova de Lisboa.

Solidoro C, Pecenik G, Pastres R, Franco D, Dejak C 1997. Modelling macroalgae (Ulva rigida) in the Venice lagoon: Model structure identification and first parameters estimation. *Ecological Modelling* **94**: 191-206.

Steele JH 1962. Environmental control of photosynthesis in the sea. *Limnology and Oceanography* **7**: 137-150.

United Nations 1992. Agenda 21. United Nations Conference on Environment and Development Rio de Janeiro, Brazil, 3 to 14 June 1992.

Vollenweider RA 1974. A manual on methods for measuring primary productivity in aquatic environments. Blackwell Scientific Publications.